NUMERICAL MODELING THE FLOOD WAVE AS A RESULT OF URKMEZ DAM FAILURE

A Thesis Submitted to
the Graduate School of Engineering and Sciences of
İzmir Institute of Technology
in Partial Fulfillment of the Requirements for the Degree of

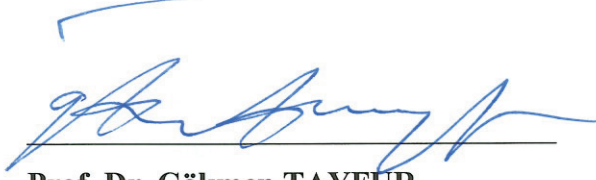MASTER OF SCIENCE

in Civil Engineering
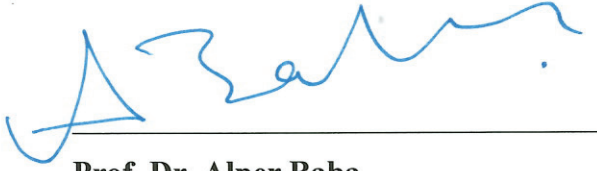
by
Gül Sümeyra ŞAHİN

December 2018
İZMİR

We approve the thesis of **Gül Sümeyra ŞAHiN**
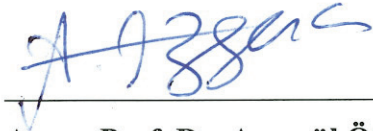
Examining Committee Members:

Prof. Dr. Gökmen TAYFUR

Civil Engineering, İzmir Institute of Technology

Prof. Dr. Alper Baba

Civil Engineering, İzmir Institute of Technology

Assoc. Prof. Dr. Ayşegül ÖZGENÇ AKSOY

Civil Engineering, İzmir Institute of Technology

25 December 2018

Prof. Dr. Gökmen TAYFUR

Supervisor, Civil Engineering,

İzmir Institute of Technology

Prof. Dr. Şebnem ELÇİ

Head of the Department of Civil Engineering

Prof. Dr. Aysun SOFUOĞLU

Dean of the Graduate School of

Engineering and Sciences

ABSTRACT

NUMERICAL MODELING THE FLOOD WAVE AS A RESULT OF ÜRKMEZ DAM

Dams are constructed to provide benefits to society, hydropower generation, including water supply management and flood control. However, floods caused by failure of a dam is quite catastrophic for lives, properties and environment. Flow models for dam break scenarios ensures crucial information about land use planning and risk managment to minimize flood losses. In this study, estimation of flood innundated areas caused by flood triggered by failure of Urkmez Dam in Izmir is carried out by using HEC-RAS one-dimensional (1D) unsteady flow routing model (full Saint Venant equations) and two dimensional model (2D) (full Saint Venant equations or Diffusion wave equations). The experimental distorted physical model provides controlling to simulations. The aim of the paper is to assess the risk of a dam failure potential by comparing performances of 1D and 2D simulations. Two models were compared considering the required data, data preparation, inundated area, flood velocity, flood depth, and flood waves.

Keywords: Dam Break, Flood routing, Flood mapping, HEC-RAS 1D model, HEC-RAS 2D model

ÖZET

ÜRKMEZ BARAJI YIKILMASI SONUCU OLUŞAN TAŞKIN DALGASININ SAYISAL MODELLENMESİ

Barajlar, insanoğlunun su ve enerji ihtiyacını karşılamak için yapılmış görkemli yapılardır. Barajlarda yönetim ve taşkın kontrolu büyük önem taşımaktadır. Taşkınlar can ve kaybına ayrıca çevresel felaketlere sebep olabilir. Taşkın kaynaklı risklerin en aza indirgenmesi için baraj yıkılma senaryolarının incelenmesi faydalı olacaktır. Bu çalışmada Urkmez Barajı'nın yıkılma senaryosu HEC-RAS programı aracılığıyla 1 boyutlu ve 2 boyutlu modeller oluşturularak incelenmiştir. Her iki modelde de kararsız akım tercih edilmiştir. Ürkmez Barajı'na ait çarpıtılmış fiziksel modelde yapılan deneyler, simülasyonlarda kontrol amaçlı kullanılmıştır. Oluşan sonuçlar taşkın haritalarında gösterilmiştir. 1 boyutlu ve 2 boyutlu modellerin performans kıyaslamasında, data hazırlama, taşkın alanları, hız ve su yükseklikleri incelenmiştir.

Anahtar Sözcükler: Taşkın, Taşkın haritaları, HEC-RAS, 1 boyutlu model, HEC-RAS 2 boyutlu model

TABLE OF CONTENTS

LIST OF FIGURES

LIST OF TABLES

CHAPTER 1

INTRODUCTION

In the last decades, sustainability has gained importance according. Engineering disciplines follow up an attentive approach due to global resources. Engineering structures should be evaluated in terms of sustainability criteria and to provide this, life cycle of structures should be identified. Life cycle refers all proses of civil structure from the cradle to grave. In other words, building, operating and terminating phases of structures should be described and included with purchasing of materials, repairment and emergency case scenario. The importance of application of life-cycle concepts is emphasized for improving life standard and public safety (Biondini and Frangopol, 2016).

Dams are vital civil engineering structures, storing water across river. Obtaining drinking water, energy generation and flood control are the main purposes of dams. The behaviors of these important structures, under risky situation, have a place in owing to avoid disaster. Also, analysis of flood on dams is matching with life-cycle concept of civil structures.

Floods are the one of the most important reason of dam breaks. Floods are natural disasters and can be identified as an overflow on land. Floods can affect daily life negatively by the causing social and economic disasters. Dam breaks also can occur due to structural instabilities.

Dams can collapse partially or completely. A dam break can result with loss of life, poverty and prevalent damage to property. In some cases, agricultural losses can be significant. An effective flood management can be achieved by prediction of flood as possible as real case. Possible losses should be determined and should be taken precautions for loss minimization.

Turkey experiences natural disasters frequently. Earthquakes, landslides, floods, erosion, droughts, rock and avalanches are faced as natural disasters. As a result of such natural disasters, there have been many life losses, injuries (social and physical) and

great economic losses. Table 1.1 gives the information about disaster occurred in Turkey between 1900-2016. (EM-Dat, 2016).

Table 1.1 Turkey Disaster List

Disaster	Frequency	Death	Incidence	Total Damage (000 $)
Earthquake	77	89,236	6,924,329	24,685,400
Extreme Temperature	7	100	8,450	1000
Flood	45	1,408	1,785,023	2,195,500
Landslide	10	293	13,481	26,000
Mass Movement	3	407	1,075	?
Storm	6	53	13,636	2,200
Forest Fire	5	15	1,150	?

Floods have pre-unidentified features due to many state variables and drive variable changing in time. In addition, representation of flood requires mathematical models. First step of flood modelling requires natural data and taking measurement. Natural data contains measurements from stream gaging station and historical data. The obtained data provides estimation for flood discharge (Kaya, 2017).

Dam break varies according to failure type. Insufficient spillway capacity, structural defects, unstable slopes, earth slides, seepage, piping, overtopping, and earthquakes are the main dam break reasons. The important part of failure is given as 38 % insufficient spillway capacity, 33%seepage and 23% piping (Bozkus 2003, Yanmaz and Beser 2005). For example, Teton Dam failed at 1976 in the US. It was 93 m high and failed 4.3 hours later after first breach. Peak flow was predicted as 42,500 m^3/s. The geological factors and seepage was the failure reason (Molu 1995).

Zeyzoun Dam failed at 2002 in Syria. It was 36 m high and 71 million m³ water flowed. At the beginning of failure, cracks were noticed (Chanson, 2009). Figure 1.1 is satellite image of the flood area. There exists no water in top image which was taken at June 3,2002. Bottom of figure shows false color image of extent of flooding. Which was taken at June 5, 2002. In the false color image, the ground is green and orange, and water is black (Source: NASA, 2002). False color is used to prefer making satellite images more comprehensive and this technique provides images that were just shades of gray. Each shade indicates different intensity of the radio emission. For example, red is assigned to the most intense radio emission and blue to the least intense emission and intermediate colors (orange, yellow, green) shows the intermediate levels of radio intensity. In the picture is given in Figure 1.1, top image shows the land without flood and sea is seen as nearly black as to radio emission. Bottom picture shows the land after flood. The flood is shown as orange.
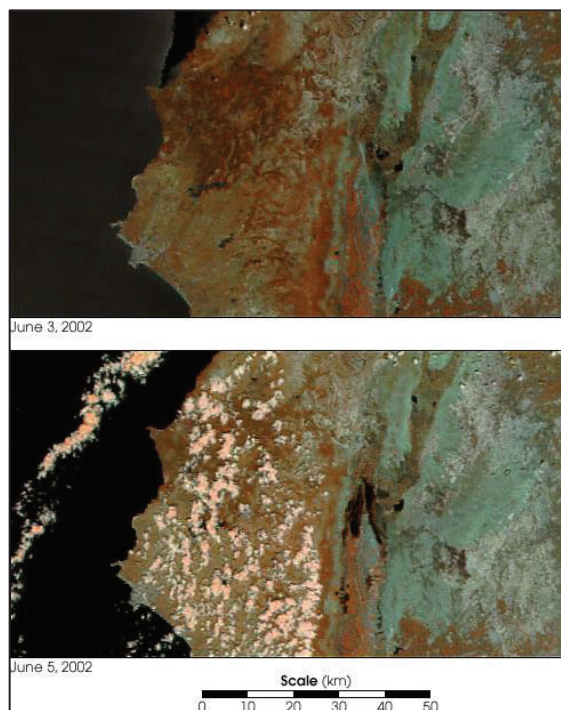
Figure 1.1: Zeyzoun Dam Failure Satellite Image (Source: NASA, 2002)

Tous dam collapsed due to heavy rain at 1982. Flow depth was 7 m and 200,000 people were influenced (Alcrudo and Mulet 2007). Tous dam failure is also one of the

3

most important failures in Spain. It is a milestone event for dam safety regulation framework (Schoolmeesters, 2008). Figure 1.2 gives an image after overtopping failure of Tous Dam. Clay core remnants can be seen between the concrete abutments (Alcrudo, 2003). Big Bay Dam collapsed in 2004 and 17.5 million m^3 water was released inundating 23 km of valley (Yochum et al 2008).

Figure 1.2: Tous Dam Failure (Source: Alcrudo, 2003)

Dam break analysis has an important point to avoid hazardous effects of flood and can help to outline of results. Dam breaks and flood can be investigated with numerical methods. Grand River flood scenario was analyzed with HEC-RAS and inundation maps were obtained for 12 different flood stages. Flood damages along the Grand River were determined in 1-dimensional case (1-D). It was stated that a flood management system can be beneficial on required stations in order to reduce damages caused by flood. Also, some suggestions are given for developing a reliable flood warning system (Lamichhane and Sharma, 2017).

Lavoie and Mahdi (2016) investigated comparison of two-dimensional (2-D) flood propagation models: SRH-2D and Hydro_AS-2D.

An experimental dataset was studied a dam break wave over a triangular bottom sill. Time step, mesh sensitivity, calibration time and water depth profiles were examined for both models. Advantages and disadvantages of modeling tools were

clarified (Lavoie and Mahdi, 2016). Almassri (2011) compared ISIS and HEC-RAS performance for dam break simulations according to numerical pysical models. Difficulties and simplicities are explained for both tools. Zhu et al (2004) reviewed embankment dam breach modeling. Dam breach models and physical studies were summarized. Lack of data on prototype embankment dam breaches, that is significant for calibration and validation of the mathematical models, were emphasised.

Physical model studies are as important as numerical studies and they should be performed as full and large scale tests (Zhu et al , 2004).

Physical models provide improving understanding of dam failure and flood propagation over actual area. The scale of model should be inadequated for some important details and experiments should ensure all field observations. By the way, smart analysis can be achieved by physical models and simulation results integration with geographic information system which is a great contribution to flood management.

Testa et al (2007) examined dam break for a simplified urban district in laboratory. In a simplified urban district, dam break was analyzed at laboratory. Concrete 50 m model represented the river with topographical details. Flood was performed with sudden rise in water level by the help of a pump. Larocque et al (2013) searched the urban flooding over New Orleans and executed the steady state flow. Flow depths and velocities were analyzed in the residential area.

Xu et al (2013) searched the effects of dam break mechanism of lanside. The effects of boulders on the top of a lanside dam, discharge channel characteristics, water flow conditions and dam size were examined. Figure 1.3 shows different water flow conditions, where the water flow is: (a) 0.1 L/s, (b) 0.2 L/s, and (c) 2 L/s.

Experimental works indicate large areas due to obtain required details and view inundated area completely after flood. Otherwise, desired flow depths and velocities could not obtained. Guney et al (2014) examined sudden partial dam break on Ürkmez area. Distorted model had 1/150 horizontal and 1/30 vertical scales. Model reservoir hold 12 m^3 water and dam body had 2.84 m width and 1.07 m height. Sudden partial collapse executed by the help of trapezoidal breach on dam body. Water levels and velocity were measured with level rod and ultrasonic velocity profiler (UVP) transducers. Buildings were represented by wooden blocks. Also important highway was constructed. The maximum flow depth was 9.88 cm on model which corresponded to 2.96 m on prototype.
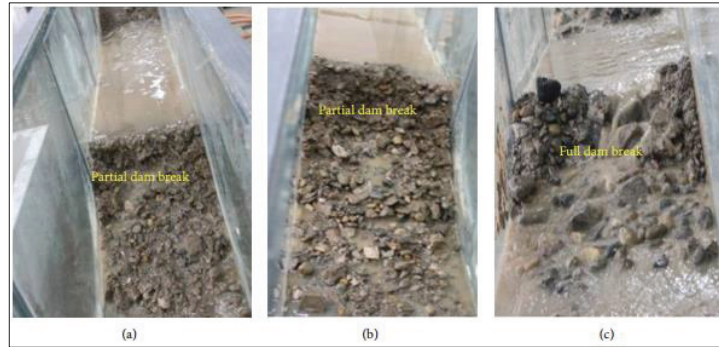
Figure 1.3: Final patterns of dam break affected by the different water flow conditions.
(Source: Zhu et al (2004)

It means that first floor of buildings could be submerged (Guney et al, 2001). Figure 1.4 displays the physical model. In literature, large scale physical model experiments are limited. Especially in Turkey, this is a good experimental study which ensure comprehending dam break on very realistic terrain. In this study, flood hydrograph is used, obtained from experimental results. Detailed information about experimental study will be given at chapter 3.

Figure 1.4: Distorted physical model of Ürkmez (Source: Guney et al,2014)

CHAPTER 2

METHODOLOGY

HEC-RAS provides that 1-dimensional (1-D) and 2-dimensional (2-D) hydraulic modelling. It was developed by the U.S. Army Corps of Engineer's Hydrologic Engineering Center. In this study, version 5.0.3 of HEC-RAS was used. Software enables performing 1-D, 2-D and 1-D combined 2-D steady and unsteady flow simulations. The HEC-RAS Technical Reference Manual (Version 5.0, 2016) has detailed and complete documentation of the 1-D modeling with underlying equations.

There exist two alternatives for 1-D flow routing: steady and unsteady flows. If a constant inflow is modeled, steady flow can be useful and depth of flow in any location does not show differences over time. If inflow is changing in time, instance, a discharge hydrograph is used, depth of flow in any location show differences over time. In this study, 1-D and 2-D unsteady simulations were investigated.

General information about the 1-D and 2-D simulations will be given in the following parts.

2.1. 1-D Model

Barre de Saint-Venant in 1871 described mathematically 1-D unsteady flow in open channels and also known as the Saint-Venant equations (Chow et al. 1988). Saint-Venant equations include mass and momentum conservation. The net rate of flow into a control volume is equal to the rate of change of storage inside the volume according to the law of conservation of mass. Conservation of mass based equations also indicate continuity equations. The net rate of momentum that enters the control volume plus the sum of all external forces.

Act on the control volume are equal to the rate of sum of momentum accordingly conservation of momentum law and where the external forces are the pressure and friction.

The continuity equation describes the preservation of mass in a given control volume. It states that the net mass flux equals the change in storage. The 1D form of the St. Venant continuity equation can be written in the following form:

$$\frac{\partial (AV)}{\partial x} + \frac{\partial A}{\partial t} - q = 0 \qquad (2.1)$$

Where Q, A is the cross section area, V is velocity and q is the lateral inflow/outflow per unit length. The first term is rate of change of flow with distance and the second term is the change of cross sectional flow area over time. The Figure 2.1 shows the control volume of the Saint-Venant equations.
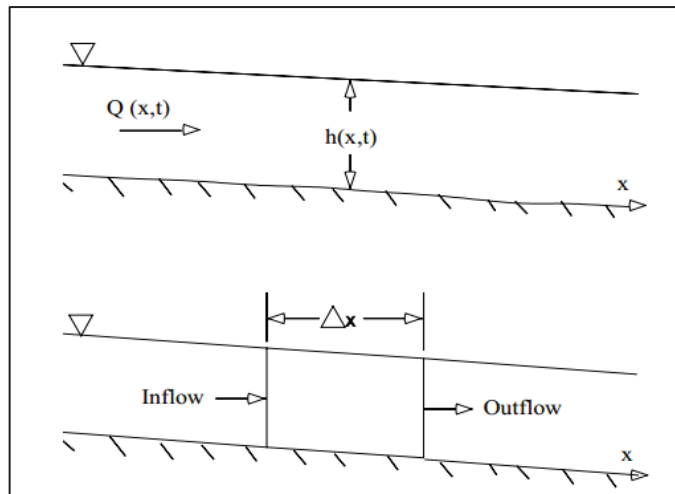

Figure 2.1: Control volume for the derivation of the Saint-Venant equations (HEC-RAS Manual 5.0.3)

The momentum equation is based on the Newtons second law of motion, stating that the sum of the forces acting on an element equals the rate of change of momentum.

The formulation of the momentum equation shows differences depending on the forces that are being considered. Taking pressure, gravity and frictional resistance into account, the 1D momentum equation can be written as:

$$\frac{\partial Q}{\partial t} + \frac{\partial QV}{\partial x} + gA(\frac{\partial H}{\partial x} + S_f) = 0 \qquad (2.2)$$

Where V is the flow velocity, g is the gravitational acceleration, H is the water surface elevation, So is the bed slope and Sf is the friction slope (can be calculated by using the Manning equation). The first term is the local acceleration term, which describes the change in momentum due to the change in velocity over time. The second term is the convective acceleration term, which describes the change in momentum due to change in velocity along the channel. The last term includes the pressure force term, which is proportional to the change in water depth along the channel, the gravity force term which is proportional to the bed slope S_0 and the friction force term proportional to the friction slope S_f.

2.1.1. Initial and Boundary Condition

Boundary should be defined at all of the open ends of the river system. Upstream boundary condition can be defined as flow hydrograph (the most common upstream boundary condition), stage hydrograph or both of them. Downstream boundary condition can be defined as the rating curve, normal depth (Manning's equation), stage hydrograph, flow hydrograph or a single-valued curve.

2.1.2. Computation of Flood Wave and Spreading

There exist two dependent (V and h) and independent parameters (x and t) according to Saint-Venant equations of 1-D open channel flow, that are partial differential equations and that only vary in longitudinal direction x. Also, there are no analytical solutions exist for these equations in the most practical applications (Maidment,1993).

The Saint-Venant equations contain the following assumptions (Maidment, 1993):

o Velocity components of other direction from flow are not taken into account.

o The water length is bigger than water depths (vertical accelerations are ignored and the pressure is assumed to be hydrostatic).

o Water level across only horizontal on a cross section

o The channel bed and banks are fixed and not movable

o The average channel bed slope is small less than 1:10

2.2. 2-D Model

2-D flow routing can be carried out using the HEC-RAS. In this study, Saint-Venant equations were used. The 2-D form of the continuity equation states, just as the 1D form, that the net mass flux into the control volume equals the change in storage in the control volume. The difference is that the mass fluxes are now calculated in two dimensions. The two dimensional continuity equation can be written as:

$$\frac{\partial h}{\partial t} + \frac{\partial (hu)}{\partial x} + \frac{\partial (hv)}{\partial y} = q \tag{2.3}$$

Where h is the water depth, u and v are the depth averaged velocities in the x- and y-direction, respectively and q is the lateral flow.

As in the 1-D case, the momentum balance is based on the principle that the sum of forces acting on an element equals the rate of change of momentum. Considering forcing from gravity, pressure and friction the 2D momentum balance equations can be written as follows. Momentum balance in the x-direction:

$$\frac{\partial u}{\partial t} + u\frac{\partial u}{\partial x} + v\frac{\partial u}{\partial y} = -g\frac{\partial H}{\partial x} + v_t - c_f u \tag{2.4}$$

The momentum balance in the y-direction:

$$\frac{\partial v}{\partial t} + u\frac{\partial v}{\partial x} + v\frac{\partial v}{\partial y} = -g\frac{\partial H}{\partial y} + v_t - c_f v \tag{2.5}$$

where h is the water surface elevation, v_t is the eddy viscosity coefficient, c_f is the friction coefficient, v and u are depth averaged velocities in the x and y directions, respectively (Brunner, 2016a). The first term in the momentum equations represents the local acceleration $\frac{\partial u}{\partial t}$ in equation 2.4, corresponding term in 2.5), the second term ($u\frac{\partial u}{\partial x} + v\frac{\partial u}{\partial y}$ in 2.4, corresponding term in 2.5) is the convective acceleration, other terms stand for the forcing from gravity, bed friction. Using the Manning's formula, the friction coefficient c_f can be expressed as following (in the x-direction):

$$S_f = \frac{n^2 g|u|}{R^{4/3}} \tag{2.6}$$

where n is Manning's roughness, g the gravitational acceleration, u the velocity in the x-direction and R the hydraulic radius. Roughness is one of the important point

for simulation. The difficulty while applying the Manning equation that there exists no exact method of selecting the n value. (Bulu, 2004). The n value would be estimated, based on the resistance to flow in a given channel (Chow, 1959). The n value is highly variable and depends on some factors like surface roughness, vegetation, channel irregularity, silting and scouring, obstruction, size and shape of the channel, and stage and discharge. Table 2.1 gives n values for a channel.

Table 2.1:Values for the computation of the roughness coefficient
(Source: Cowan,1956)

Channel Condition			Values
Material involved	Earth	n_0	0.020
	Rock		0.025
	Fine Gravel		0.024
	Coarse Gravel		0.028
Degree of irregularity	Smooth	n_1	0.000
	Minor		0.005
	Moderate		0.010
	Severe		0.020
Variations of channel cross	Gradual	n_2	0.000
	Alternating		0.005
	Alternating		0.010-0.015
Relative effect of obstructions	Negligible	n_3	0.000
	Minor		0.010-0.015
	Appreciable		0.020-0.030
	Severe		0.040-0.060
Vegatation	Low	n_4	0.005-0.010
	Medium		0.010-0.020
	High		0.025-0.050
	Very High		0.050-0.100
	Minor		1

Cowan (1956) enhanced a method for estimating the value of n as:

$$n = (n_0 + n_1 + n_2 + n_3 + n_4) * m \qquad (2.7)$$

Where the n_0 represents a basic value for channel containing natural materials, n_1 represents the surface irregularities, n_2 represents variations in shape and size of the channel cross section, n_3 represents obstructions, n_4 represents vegetation and flow condition and m represents a meandering correction factor (French, 1994).

By using HEC-GeoRAS interface, Manning roughness values are determined according to flood area and Table 2.2 shows the values.

Table 2.2 Manning roughness coefficients

OBJECTID	LUCode	N_VALUE	HydroID
1	Veg	0.025	54
2	Obs	0.03	55
3	Obs	0.027	56

2.2.1. Initial and Boundary Conditions

Boundary conditions can be defined in five different types such flow hydrograph, stage hydrograph, normal depth, rating curve and precipitation. In this study flow hydrograph was used as a boundary condition.

Initial conditions can be defined in two ways. The most common way is entering flow data. Second way is using previous run as an initial condition, by this way programme can accept as a subsequent run. In this study, very small flow was described as initial condition.

2.2.2. Computation of Flood Wave and Spreading

2-D modeling gives better results for the very wide and flat flood plains such that when the flows goes out into the overbank area the water will take multiple flow paths and have varying water surface elevations and velocities in multiple directions.

2.3. Modeling Procedure of HEC-RAS 1-D

HEC-RAS requires two types of data: flow data and geometric data, both for 1D and 2D modelling. Geometric data can be defined manually as well as processed. HEC-GeoRAS is a geographic information system interface which provides import file that can be prepared for HEC-RAS and create maps. Figure X shows the basic flowchart between HEC-RAS and HEC-GeoRAS.
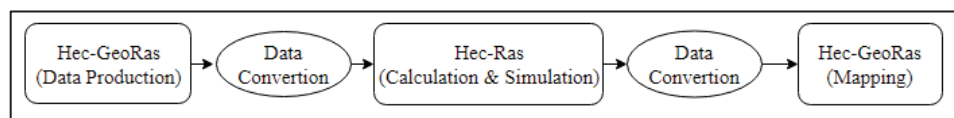

Figure 2.2: Workflow between HEC-RAS and HEC-GeoRAS

Geometric data like cross sections, river, inline structure, channel banks etc. can be created by using on HEC-GeoRas. Hec-GeoRas is a set of ArcGIS tools for processing geospatial data for use with HEC-RAS. The produced data exported must be compatible with HEC-RAS for using the geometric data. After both geometric and flow are described in HEC-RAS, simulation can be achieved. Simulation results should be exported accordingly GIS data which is data conversion step. The exported data (sdf file) can be used Hec-GeoRas while mapping the flood/flow. The Figure 2.3 shows the mapping process.

```
          ┌──────────────────────┐
          │ Start an ArcGIS Project │
          └──────────────────────┘
                     │
                     ▼
          ┌──────────────────────┐
          │ GIS Data Development  │
          └──────────────────────┘
                     │
                     ▼
          ┌──────────────────────┐
          │   Generate RAS GIS    │
          │     Import File       │
          │   (RASImport,sdf)     │
          └──────────────────────┘
                     │
                     ▼
          ┌──────────────────────┐
          │     Run HEC-RAS       │
          └──────────────────────┘
                     │
                     ▼
          ┌──────────────────────┐
          │   Generate RAS GIS    │
          │     Export File       │
          │   .RASExport.sdf      │
          └──────────────────────┘
                     │
                     ▼
          ┌──────────────────────┐
          │     RAS Result        │
          │     Processing        │
          │     RAS Mapping       │
          └──────────────────────┘
```
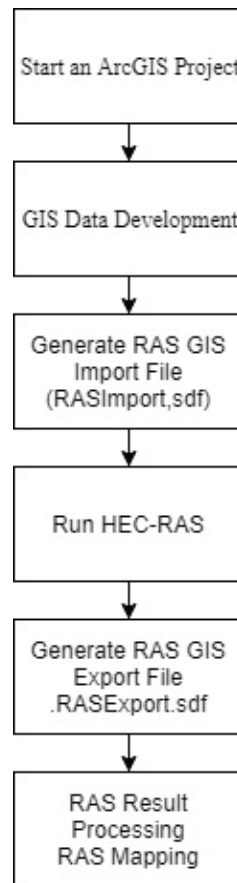
Figure 2.3: Workflow between HEC-RAS and HEC-GeoRAS - 2

Visualization and analyzation start with ArcGIS. Before the Hec-GeoRAS process, study area should be defined at ArcGIS. The produced data can be used for simulation. After simulation, exported file can be used in Hec-GeoRAS and ArcGIS for the detailed visualization.

Flow data consist of steady and unsteady flows. Unsteady flow data requires boundary conditions as well as initial conditions. Geometric data includes storage data, river system data, cross sections data, friction losses and hydraulic structure data (bridges, spillways, culvert and weir etc.). Hec-GeoRAS provides convenience to prepare geometric data and data processing. Data is produced by the help of digital elevation model (DEM) of the area. The resolution accuracy of DEM increases the accuracy of simulation. Figure 2.4, shows the cross sections obtained by the help of HEC-GeoRAS and creating model component on HEC-RAS. Channel, left and right banks and river are blue, red and green lines, are found by Hec-GeoRAS. River should

be defined from upstream to downstream. Horizontal green line is the cross section which flood will occur on. Each flood component has an identification number which is called hydro id. With the help of this ids query can be done more quickly in database. Small screen in Figure 2.4 shows the cross section profile of 5th cross section in upstream area.
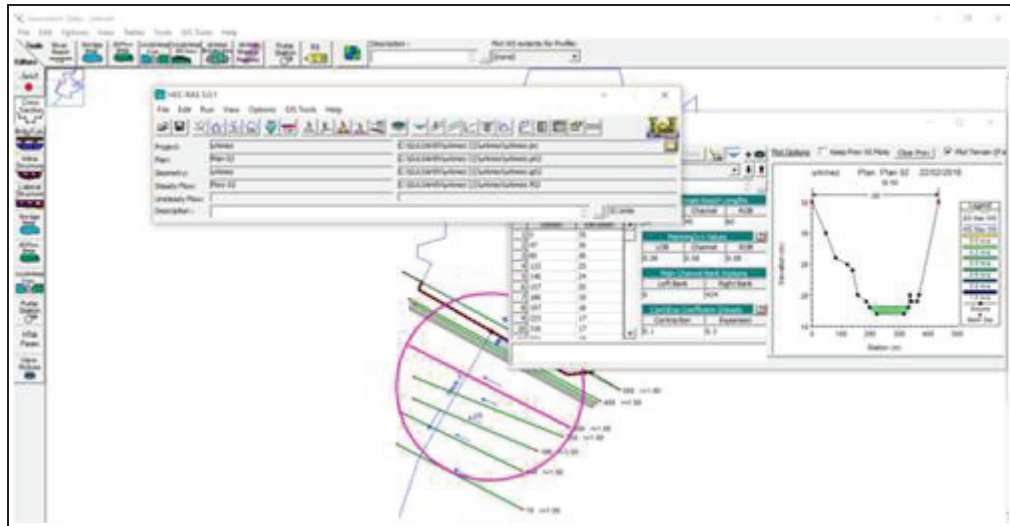

Figure 2.4 Cross Sections for HEC-RAS 1D

After geometric data is completed, flow data should be identified. The unsteady flow data consists of boundary and initial conditions.

In Figure 2.5 unsteady flow data entry window can be seen. Boundary condition is identified as a flow hydrograph. Also, there are some other alternatives for boundary conditions like normal depth, precipitation and rating curve etc. Figure 2.5 shows the unsteady data window for 1D model and it was chosen as the normal depth.

Once the geometric data and flow data are completed, then the next step is to run the model. Figure 2.6 show the running options for 1D model. Geometry and flow file should be specified and the option for output can be chosen from among the geometry preprocessor, unsteady flow simulation, post processor and floodplain mapping. Geometry preprocessor checks the geometry stability. Unsteady flow simulation choice indicates the simulation according to given flow data. Post processor provides managing and exporting model results. Simulation time should be defined in the time window and

the computation settings provide the intended output interval for computation, mapping output and hydrograph output.
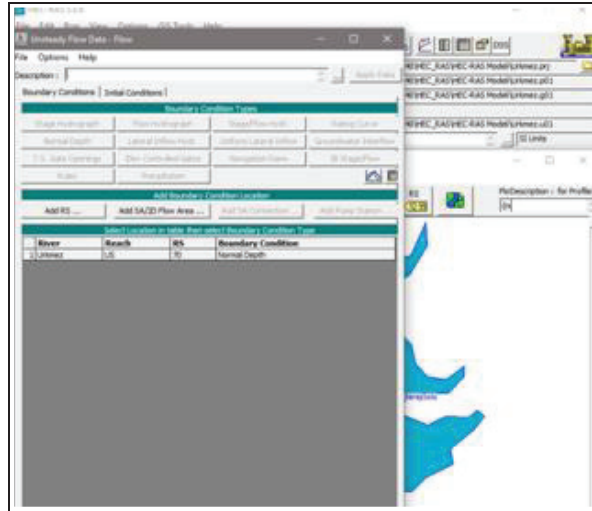

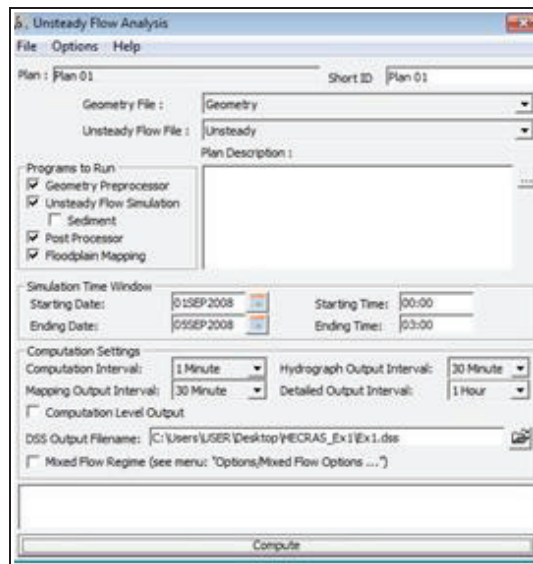Figure 2.5 Flow data screen on HEC-RAS

Figure 2.6 Computation screen on HEC-RAS

After the computation results can be exported to Hec-GeoRAS. HEC-RAS file format is sdf and it should be converted to xml because Hec-GeoRAS can work with only it. Then, the detailed maps can be created in GIS environment. Figure 2.7 shows the flood map after 1D model run and cross section view.
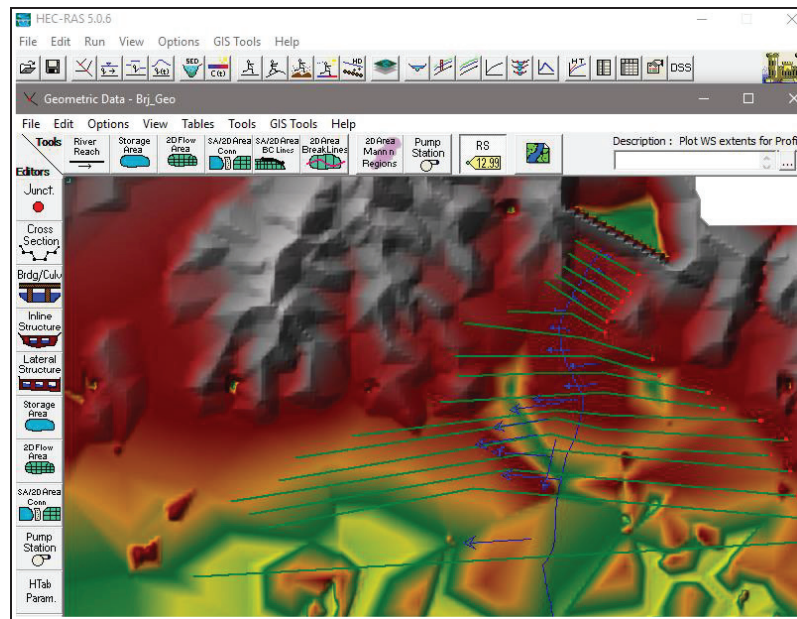

Figure 2.7 Computation screen on HEC-RAS-2.

2.4. Modeling Procedure of HEC-RAS 2-D

HEC-RAS 2D modelling requires 2D flow area and flow data. In 2D modelling, terrain represents inundation area but inundation area in 1D modelling was implied with cross sections. Terrain data is known as a series of points, included x –y and related –z values and it is very important for sufficient detailed hydraulic model. The quality of terrain data (comes from many different sources, formats and level of details) affect the quality of model and simulations. Figure 2.8 shows the computational mesh of flood area. Computational mesh was created according to flood plain and terrain. Instead of studying on infinite terrain, discretized terrain which is called computational mesh allows the computation can be made over a finite domain. The pink line in Figure 2.8 indicates the flood area.
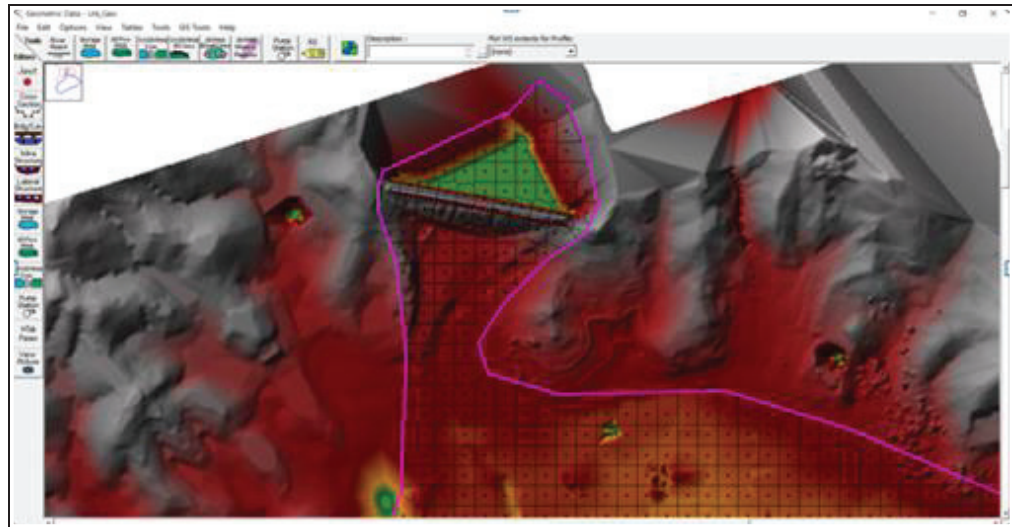
Figure 2.8: Computational Mesh Detailed Subgrid Terrain Data

Figure 2.9 shows the flow data screen for 2D model. The flow chart of the methodology is illustrated in Figure 2.10. Topographic map of the area is used in Arc-GIS for obtaining details. DEM was created. By the using DEM on Hec-GeoRAS, geometric model components like stream centerline, flow direction, cross sections of 1D model was obtained. In 2D model Hec-GeoRAS was used for obtaining 2D mesh for flood area. Then flow data was defined in both 1D and 2D models. Then, there was no missing data for simulations.

After dam break calculation, flood maps were created by the help of Hec-GeoRAS. The obtained results for dam breach analysis were compared for 1-D and 2-D simulations. Two models were compared with regard to data for simulation, data preparation time, inundated area, flood velocity, flood depth and travel time of flood waves. Floods are examined with 1-D and 2-D models by using HEC-RAS. Inundated areas and velocities were determined by using HEC-RAS and both 1-D and 2-D simulations are compared in this study. Boundary and initial conditions, other important parameters were specified according to experimental studies of site.
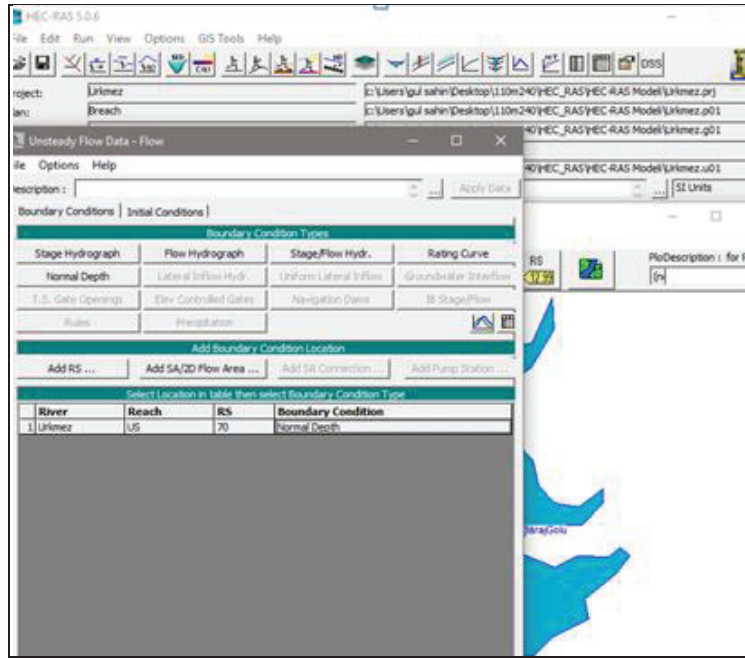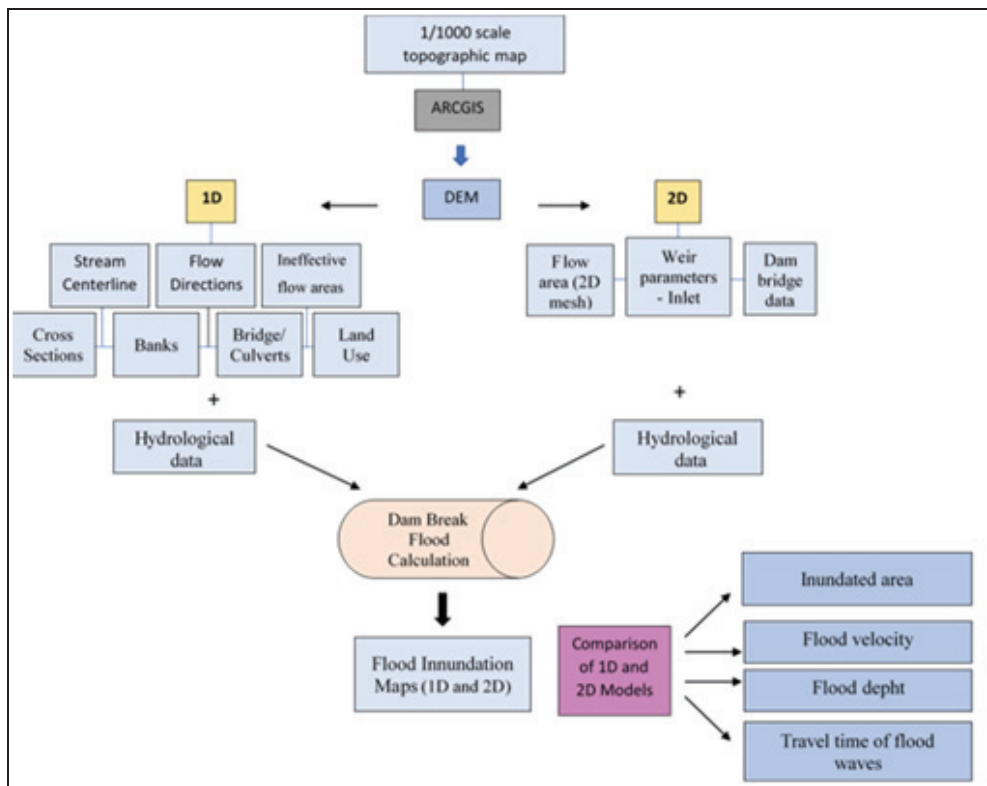
Figure 2.9: Flow Data HEC-RAS 2D

Figure 2.10: Flow Chart Of Methodology

CHAPTER 3

PHYSICAL MODEL AND SIMULATION DATA

3.1. Physical Model

Physical model studies are valuable for better understanding the dam breaks. Especially, if the topography is represented in model, it gives the opportunity to calibration for simulation.

In this study, physical model results were used as a conformity evaluation. The physical model of Ürkmez Dam, including its reservoir, dam body and downstream area, was constructed in the open space area of Hydraulic Lab of Dokuz Eylül University. The topography, the creek, the highway and settlement area were reflected in the model. The physical model was distorted as the horizontal scale of 1/150 and vertical scale of 1/30. So, the distortion ratio was 1/5. Velocity scale was $V_p=5.5V_m$ and time scale was $t_p=27.5t_m$.

By the help of maps which have vertical scale 1/1000 and horizontal scale 1/5000, 200 meters cross sections were obtained. If horizontal scale $L_{r,x} = 1/150$ and vertical scale $L_{r,z}= 1/30$ are taken into account, following scales are obtained:

Distortion Ratio,

$$D(L_r) = S(L_x)/S(L_z) = 1/5$$

Froude number needs to be satisfied for both the prototype and the physical model and thus;

$$\frac{V_m}{\sqrt{gL_{zm}}} = \frac{V_p}{\sqrt{gL_{zp}}}$$

(3.1)

Equation (3.1) can be written as follows:

$$\frac{V_m}{V_p} \frac{\sqrt{L_{zp}}}{\sqrt{L_{zm}}} = 1$$

(3.2)

Re-writing Equation (3.2) as;

$$S(V) = S(L_z)^{05}$$

(3.3)

Where,

$$S(V) = \frac{V_m}{V_p}$$

and

$$S(L_z)^{0.5} = \sqrt{\frac{L_{zm}}{L_{zp}}} .$$

This implies that $V_p = 5.48 \ V_m$. For example; measured 10 m/s velocity in the distorted model would correspond to 54.8 m/s in the actual field.

Strouhal number should be satisfied for the distorted physical model and the prototype (Yalin 1971):

$$\frac{V_m T_m}{L_{xm}} = \frac{V_p T_p}{L_{xp}}$$

(3.4)

Equation (3.4) can be expressed as follows:

$$\frac{V_m}{V_p} \frac{T_m}{T_p} \frac{L_{xp}}{L_{xm}} = 1$$

(3.5)

Equation (5) can be stated as:

$$S(V)\,S(T) = S(L_x)$$

(3.6)

where $S(T) = T_m/T_p$ and $S(L_x) = L_{xm}/L_{xp}$.

Solving Equation (3.6) for S(T) first and then making the use of Equation (3) would yield the time scale as follows;

$$S(T) = S(L_x)/S(L_z)^{0.5}$$

(3.7)

According to Equation (7), the time scale for the distorted model becomes $S(T)=\frac{\sqrt{30}}{150}$. In other words, $T_p = 27.38\ T_m$. For example, a flood wave front reaching a downstream in 13 s in the distorted physical model experiment would correspond to about 6 min in the actual field.

Geometric characteristics of the Ürkmez Dam and the physical model can be seen at Table 3.1.

Table 3.1 Geometric Characteristics

Characteristics	Prototype	Physical Model
Crest lenght	426 m	2.84 m
Crest width	12 m	0.08 m
Dam height from base	32 m	1.07 m
Lake volume at minimum level	375,000 m^3	0.556 m^3
Lake volume at maximum level	8,625,000 m^3	12.778 m^3
Lake volume at normal level	7,950,000 m^3	11.778 m^3
Lake active volume	7,575,000 m^3	11.222 m^3

The model is located at Dokuz Eylül University (DEU) Laboratory. The area was leveled for model and concrete was poured and 300 mm diameter 2 pipes were placed due to drainage of water. Sides of area were bonded. The model cross sections of Ürkmez river, dam reservoir and downstream area were drawn to represent the topographic characteristics. Cross sections in every 50 m in the downstream were obtained from detailed maps. After cross sections were drawn, they were manufactured from metal sheets by welding. Figure 3.1 shows construction phase of model site. And Figure 3.2 shows (a) sketched 1-1 cross section and (b) manufactured cross section. Metal cross section were welded with means of nivo. Figure 3.3 illustrates the metal skeleton of model.

After all cross sections were located, area was poured with concrete and surface was treated due to prevent any filtration. Dam reservoir can be seen in Figure 3.4.

Residential district was made with wooden blocks. Building were represented with wooden blocks and the dimensions were 5*10 cm^2 accordingly distortion scale. In the study area, buildings had typically 3 m story height. If the vertical scale ($L_y = 1/30$) was considered, one story house should be represented 10 cm height in the model. All wooden blocks were screwed and sticked. Also, important highway was placed in model. Figure 3.5 illustrates the downstream area, including residential district.
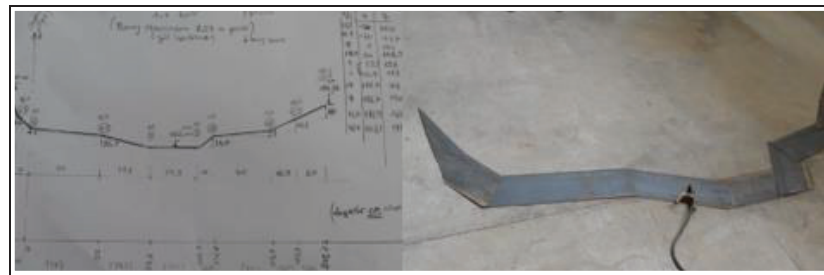
Figure 3.1 Construction of Model Site

Figure 3.2 Sketched and Manufactured 1-1 Cross Section

Figure 3.3 Metal Skeleton of Dam Site

Figure 3.4 Dam Reservoir

Figure 3.5 Downstream Area

Dam body was performed with a trapezoidal section. Dam body could be lifted up due to create dam break by the help of a pump. By the controlling dam body, desired scenarios could be achieved like partial or sudden dam breaks. Figure 3.6 shows the trapezoidal dam body and sketch of it.
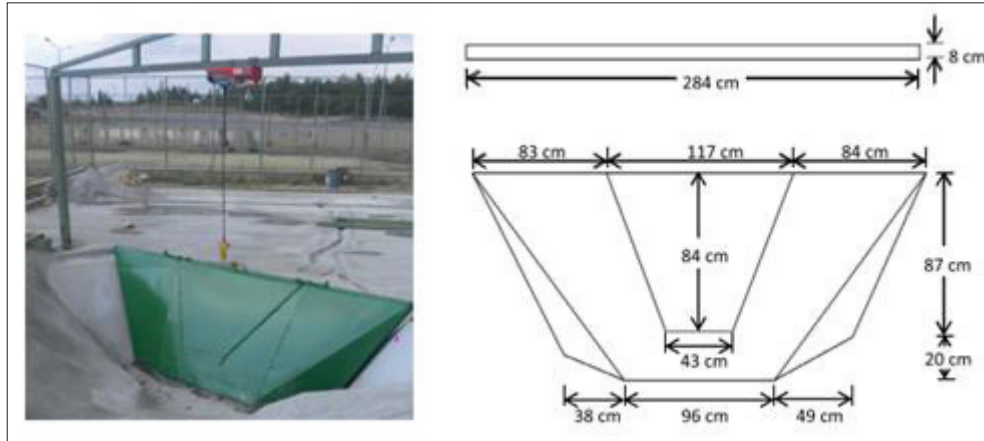
Figure 3.6: Dam body with dimensions

To measure flow velocity and water depths, e+ WATER L level rods and ultrasonic velocity profiler (UVP) transducer were used during experiments. Water level rods were located in lake and downstream area. Three of them (L1, L2, L13) were placed in lake for observing water level of lake and the others (L2, L3, L4, L5, L6, L7, L8, L9, L10, L11) were placed in downstream area to observe water depths at downstream area. The velocities were to place at 4 points (V2, V3, V4, V7) in downstream area. Figure 3.6 shows orientation of UVP transducers, where α was vertical in cross-sectional view and β was horizontal in planar view and locations of level rods and UVP transducers are shown in Figure 3.7 and 3.8 (Guney et al, 2014).

After each experiment, discharge, water levels and velocities were measured to comparison. Average discharge, was obtained from experiments was nearly 0.35 m^3/s, water levels increased at 5.5 cm at L10 and velocities at point V3 (near dam) reached nearly 7 m/s.

Flood propagation was recorded during the experiments. Flood reached the area close to dam body in 2 s (nearly 1 min in prototype), at the residential district and highway in 4 s (nearly 2 min in prototype and at sea cost in 8 s (nearly 4 min in prototype). Figure 3.9 depicts the flood propagation.

This model investigated the flood propagation nearly 6.5 km^2 in prototype and model sit 300 m^2 area in laboratory. Peak discharge, obtaining from experiments was 0.35 m^3/s equal to 8.75 m^3/s in prototype. The obtained discharge hydrograph and water level was used as boundary of storage area (flow hydrograph and initial elevation) on

simulations. Experimental discharge hydrograph was extended to prototype accordingly distortion scale. Figure 3.10 shows the used boundary condition in simulation.
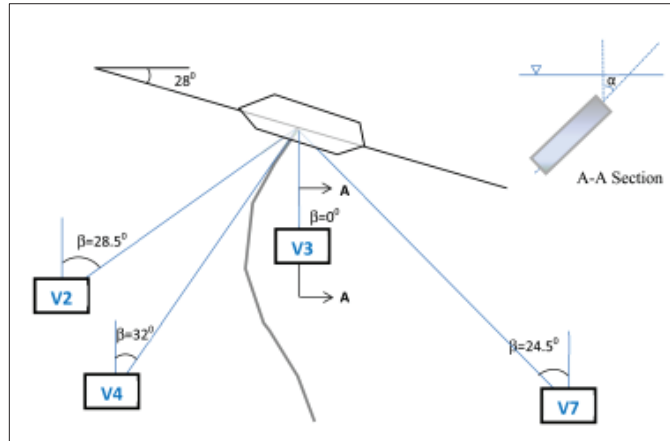

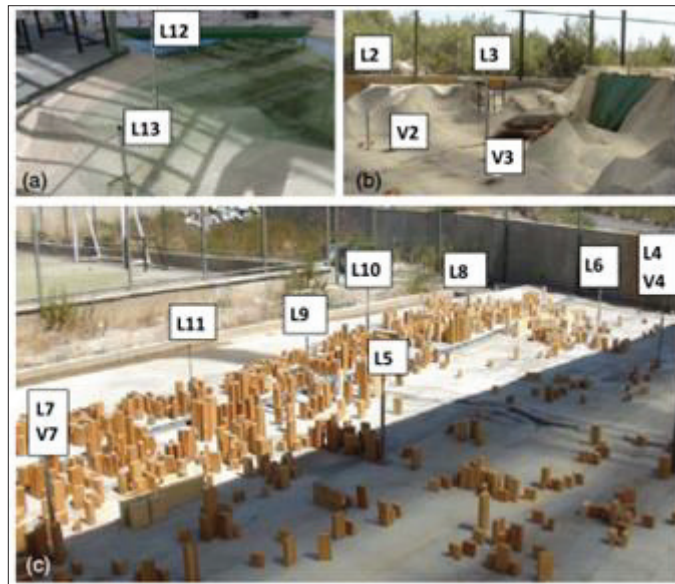Figure 3.7 Orientation of UVP Transducers (Guney et al, 2014)

Figure 3.8: Locations of Level Meters and UVP Transducers: (a)dam reservoir (b) downstream part of dam (c) residential area (Source: Guney et al, 2014)
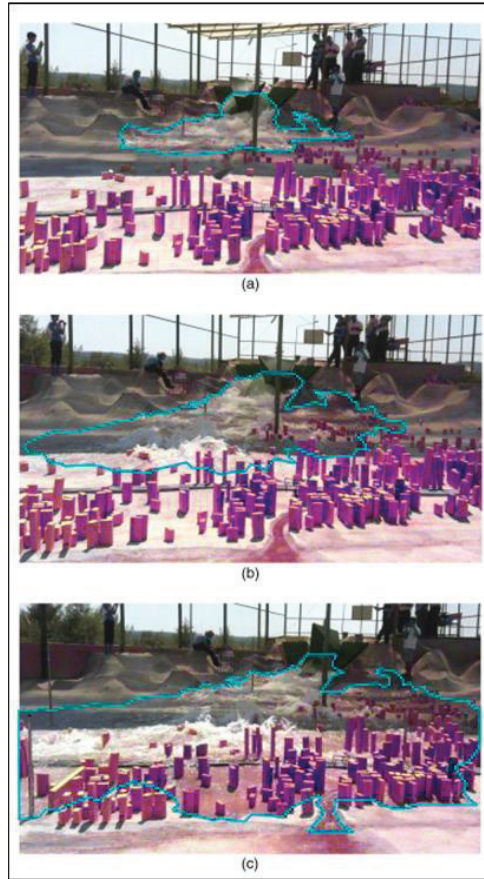
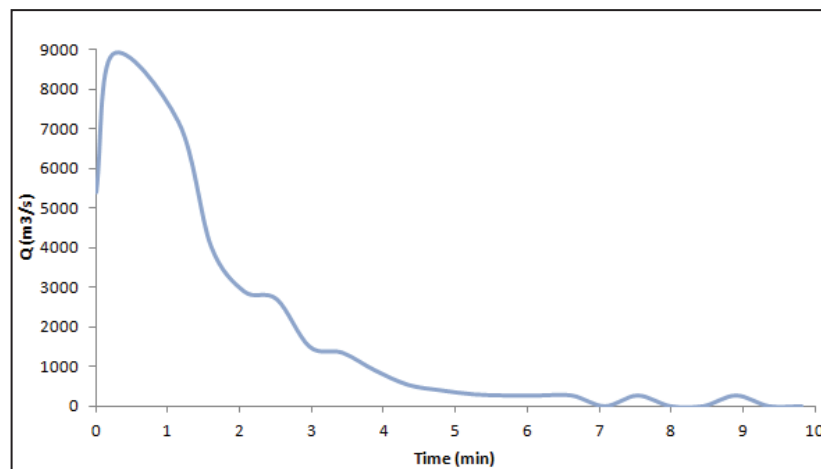Figure 3.9: Flood Propagation at (a) 2s; (b) 4 s; (c) 8 s of the experiment

(Source: Guney et al, 2014)

Figure 3.10: Boundary Condition (Discharge Hydrograph)

To sum up, experimental results was lead the simulation. Flood hydrograph was used by assembling actual size and water depths and velocities were used as a part of calibration of models. It will be discussed in Chapter 4.

3.2.   Simulation Data

Topographic map scale 1:1,000 (UTM Zone 27 / WGS 84 3º) was used for creating DEM. Data pertaining to the dam and the reservoir were provided from the State Hydraulic Works (DSI). Reservoir volume-elevation curve was provided from DSI. Model DEM was about 10 cm spatial resolution for Ürkmez Basin. DEM is used for both 1D and 2D model and land usage information were evaluated for both models. Figure 3.11 illustrates the settlement of flood area. (Settlement maps was provided by General Directorate for State Hydraulic Works)

While cross section was created in Hec-GeoRAS for 1D model, z values were extracted from Triangular Irregular Network (TIN) surface. Also, geometric data like the stream centerline, banks, flow direction, land use, bridges/culverts, ineffective flow areas were created by using HEC-GeoRAS in GIS (Geographical Information Systems) environment. But flow area of (computational mesh), weir parameters - inlet, dam bridge data were created in HEC-RAS for 2D model. Used data and usage purposes are shown in the Table 3.2.
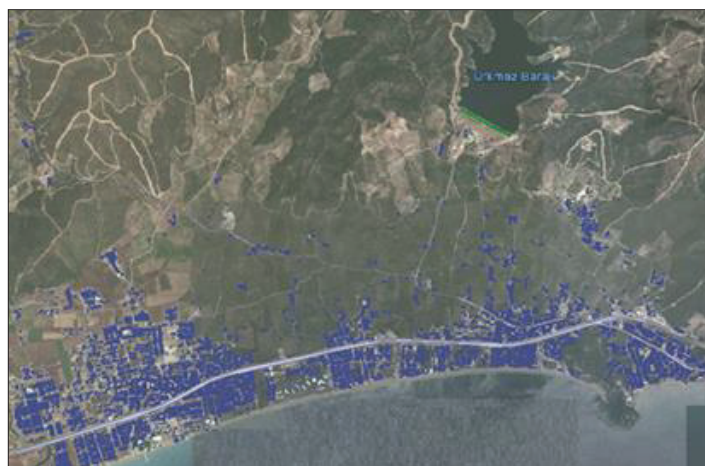

Figure 3.11: Settlement of Study Area

(Source: General Directorate for State Hydraulic Works, Google)

Table 3.2: Used Data and Purposes

Data	Purpose	1D	2D
Topographic map	Creating DEM	+	+
	Determining basin characteristics		
	Flood boundary		
Satellite image	Determining entities on the flood area	+	+
	Determining entities under risk		
	Determining roughness parameter		
	Correction of flood scenario		
River Alignment	Flood and determining effects	+	
Cross sections	Flood and determining effects	+	
Flood Area	Flood and determining effects		+

CHAPTER 4

MODEL APPLICATION TO ACTUAL ÜRKMEZ DAM

4.1. Study Area

Ürkmez dam was built for drinkable water supply and irrigation. Dam is located at 3 km north of Ürkmez city. Construction of Ürkmez Dam was completed at 1990 by General Directorate for State Hydraulic Works and started on irrigation. At 2004, municipal water treatment plant was built by Provincial Bank. Topographical map of area was supplied by the General Directorate for State Works and IZSU Administration.

Figures 4.1 and 4.2 show the location of Ürkmez, Ürkmez Dam and Ürkmez Town.

Figure 4.1: Location of Area (Source: Google)

Figure 4.2: Flood Area (Source: Google)

Figure 4.3 indicates the study area, which is nearly 30 km^2. There existed mandarin trees as vegetation. The settlement is near by the seaside. The main road passes behind the settlement.
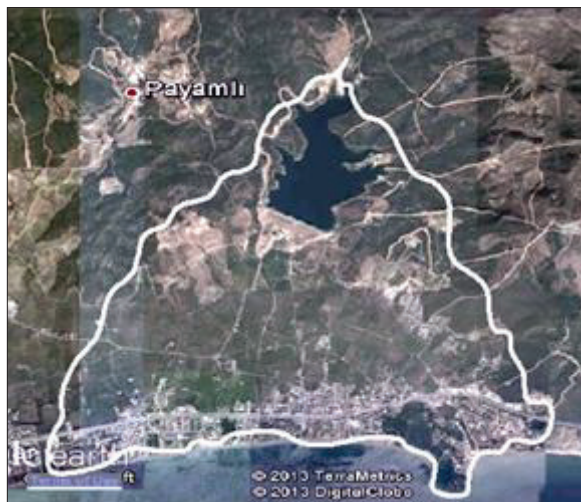
Figure 4.3: Study Area (Source: Google)

Digital Elevation Model is given in the Figure 4.4. The area has not narrow or deep basin, area enlarges to the sea. Top of the picture indicates the dam reservoir

and upstream side and bottom of picture indicates the downstream of area which merges with sea.
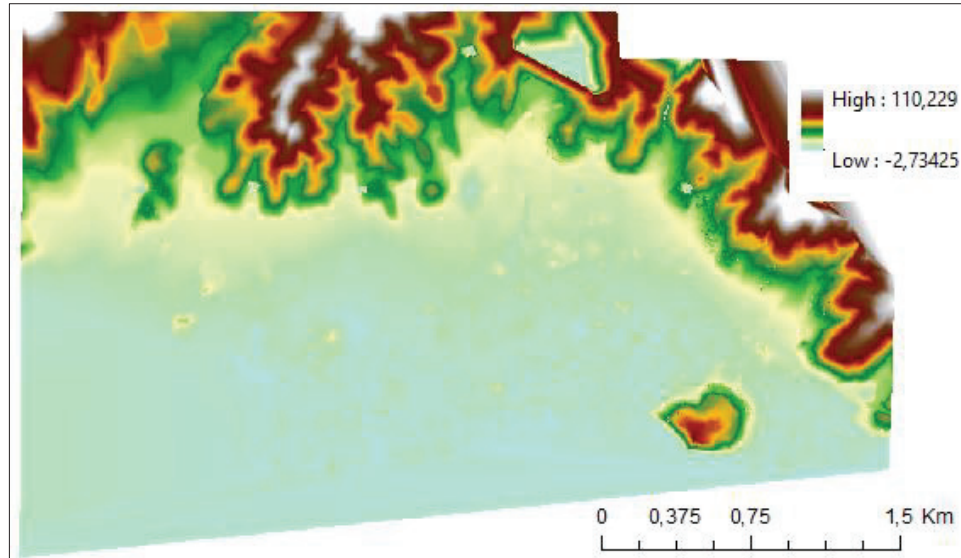
Figure 4.4: DEM of Study Area

4.1. HEC-RAS 1D Model Application

According to 1D simulation, inundation area is represented with cross sections. The cross sections should be selected correctly. Data processing is an important step. River length is 1.6 km from body dam to sea and there exists 17 cross sections in the model. Space between 2 cross sections changed between 80 m-110 m. To demonstrate the flood correctly, cross sections were selected reflecting geometry. Figure 4.5 shows cross sections, river bed and river.

Representing more cross sections provides reflecting the geometry more in detail however, short distance between cross sections causes overestimation. This can cause steep flood wave, shows the model instability (Brunner, 2016).

As upstream boundary condition, flood hydrograph was used and flood hydrograph was determined by the help of physical model. According to physical model

peak flood wave from upstream was 0.35m^3/s and it was equal to 7,800m^3/s in prototype.
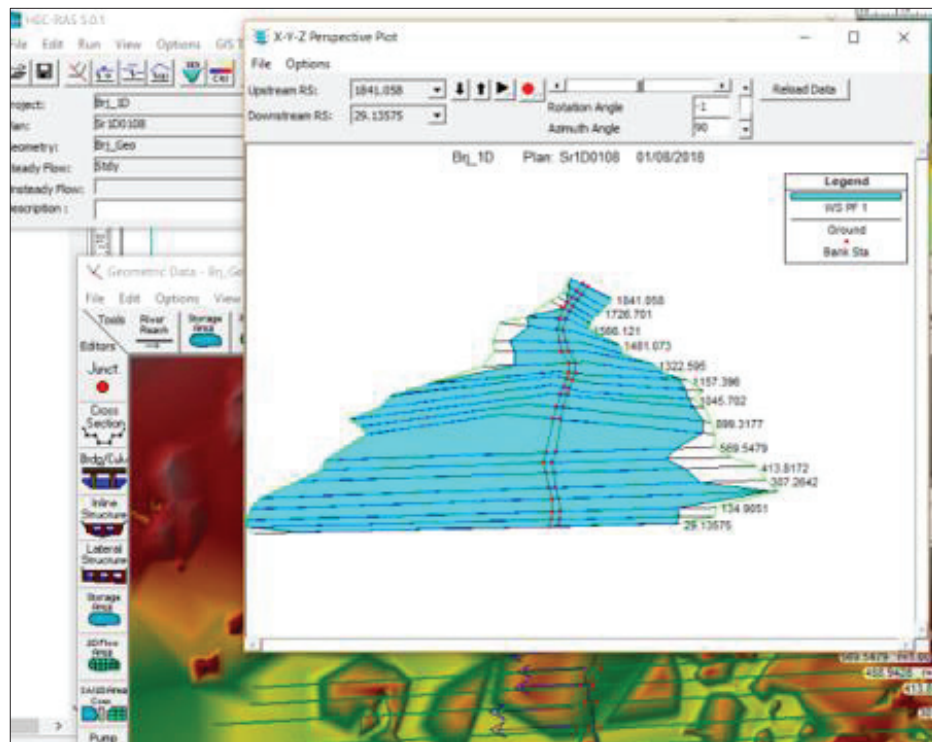
Figure 4.5: Study Area(1D)

The unsteady simulation run at a sunny normal day and there was no precipitation so initial condition was normal depth for the Ürkmez River. The velocity and water depth results of unsteady 1D simulation had not a perfect overlapping with physical model results. The reasons could be roughness coefficient. In the model, 3 different roughness coefficients were identified due to representation of the vegetation, settlement and other (wild) areas. However, the physical model was not able to represent the different land use.

Figures 4.6 and 4.7 shows, the depth and velocity results. Simulation depth and velocity values are higher than the results of experiment. The highest depth was 2.6 m at experiment and 7.53 m at simulation. The highest velocity was 2.26 m/s at experiment and 13.6 m/s at 1D simulation. Both velocity and depth were analyzed at Location 4 (given in Chapter 3) right downstream area because experimental study had accurate results.
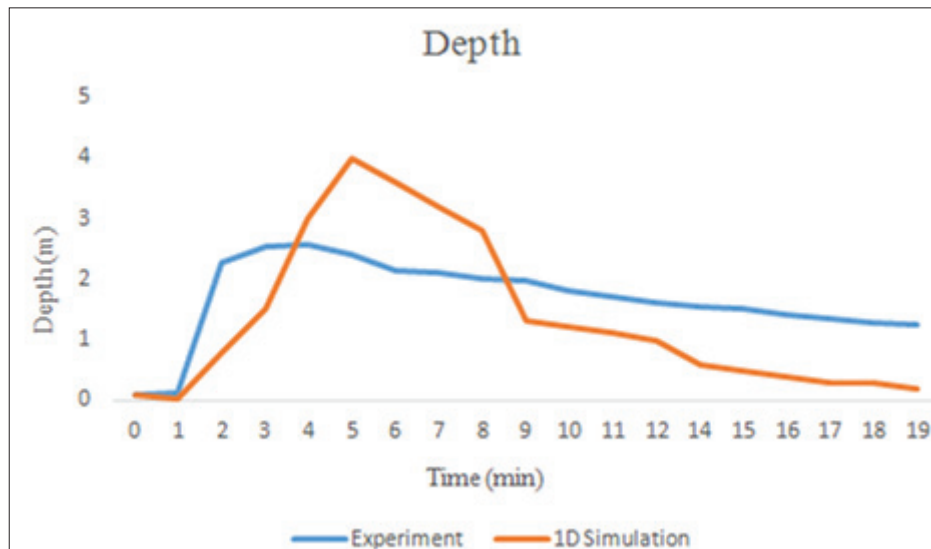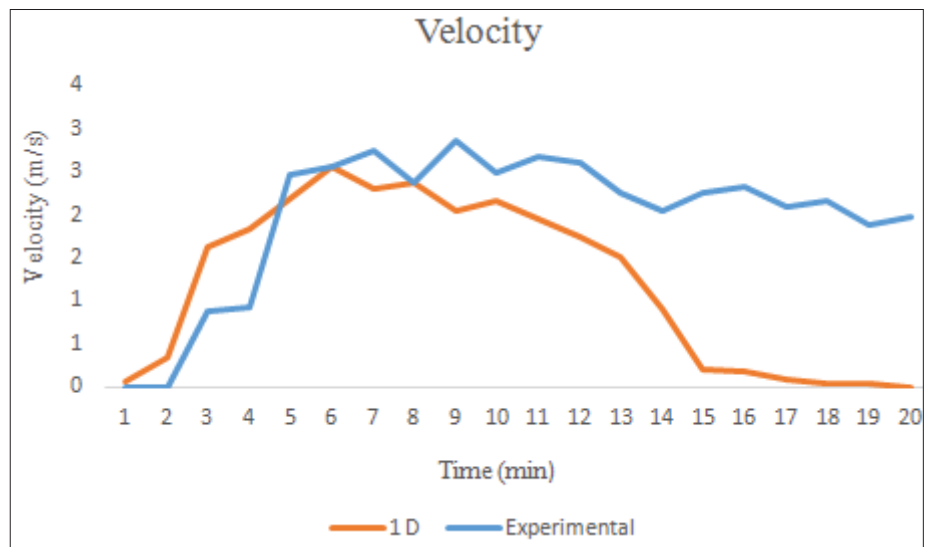
Figure 4.6: Depth Comparison

Figure 4.7: Velocity Comparison

The Figure 4.8 represents the water depths after 1D simulation at 2nd minute. Depths varied 1.94 m to 7.53 m. Water could not reach some higher elevated area. The highest water depth encountered right in front of the dam gate. 280 ha area was inundated. Water propagation was given in the Figures from 4.9 to 4.13.
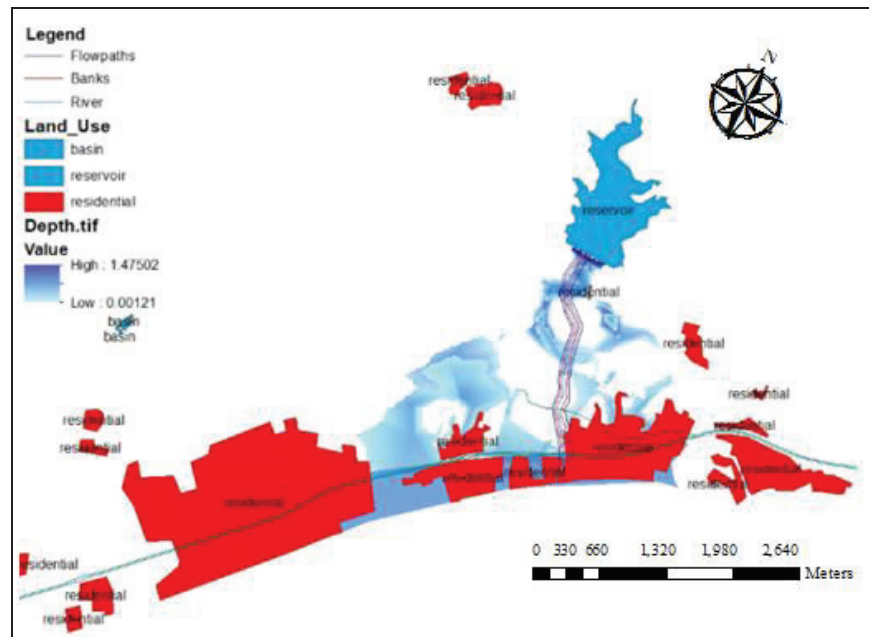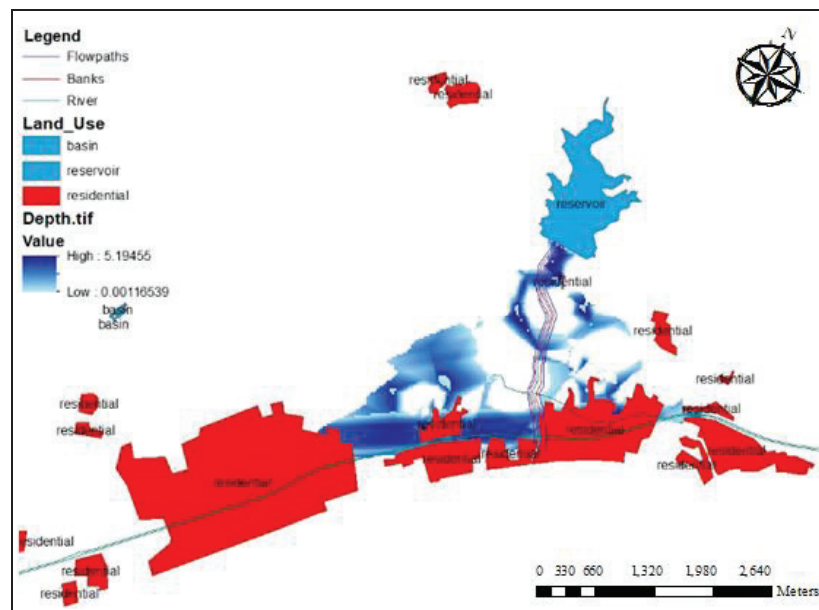
Figure 4.8: Water Propagation at 15 sec
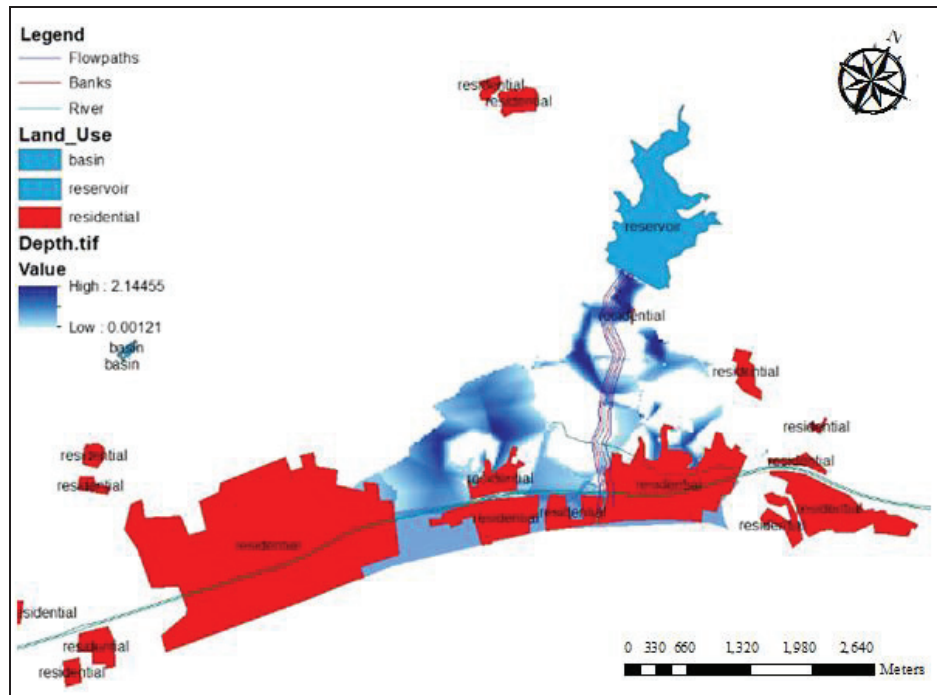

Figure 4.9: Water Propagation at 25 sec

Figure 4.10: Water Propagation at 40 sec
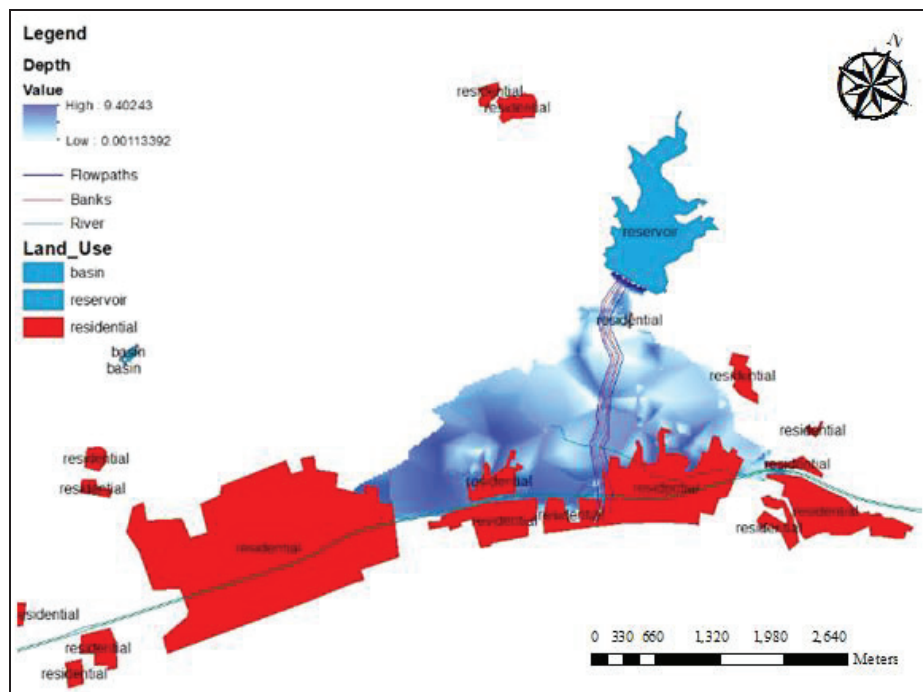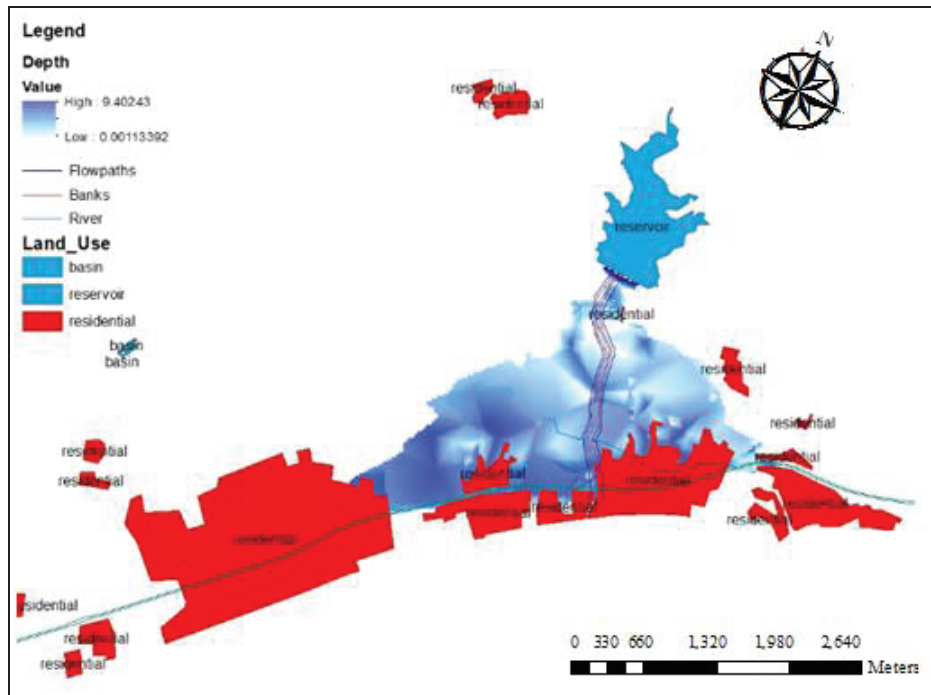

Figure 4.11: Water Propagation at 1.5 min

38

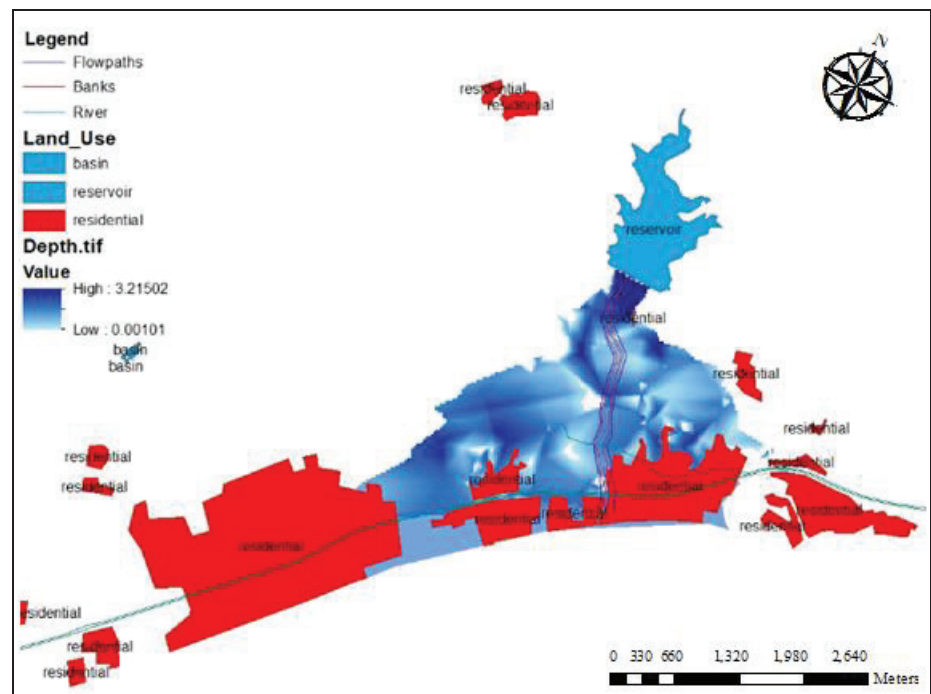Figure 4.12: Water Propagation at 2 min

Figure 4.13: Water Propagation at 2.5 min

The velocity varied 0.018 m/s to 13.6 m/s. The maximum velocity occurred at 1.5 minutes. Detailed water velocity profile given in Figure 4.14.
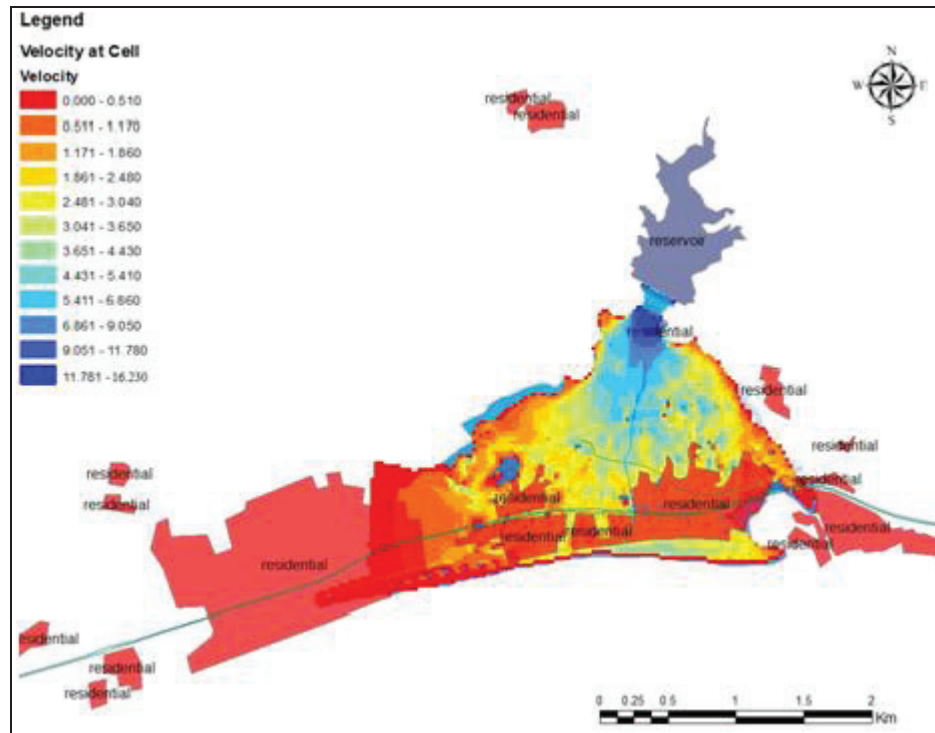

Figure 4.14: Detailed Velocity Profile

4.1. HEC-RAS 2D Model Application

According to 2D simulation, inundation area is represented with a computational mesh. To represent the inundation area cell size should be chosen correctly and sufficiently. If the cell size increases, simulation time increases. If the cell size is as big as not containing sufficient geometric information, simulation results could occur without desired detail. The studied area in HEC-RAS nearly 30 km^2. Cell size was chosen 10x10 m so there were nearly **30,000 cells in the computational mesh**, representing the inundation area. Figure 4.15 shows the 2D inundation area and dam reservoir.
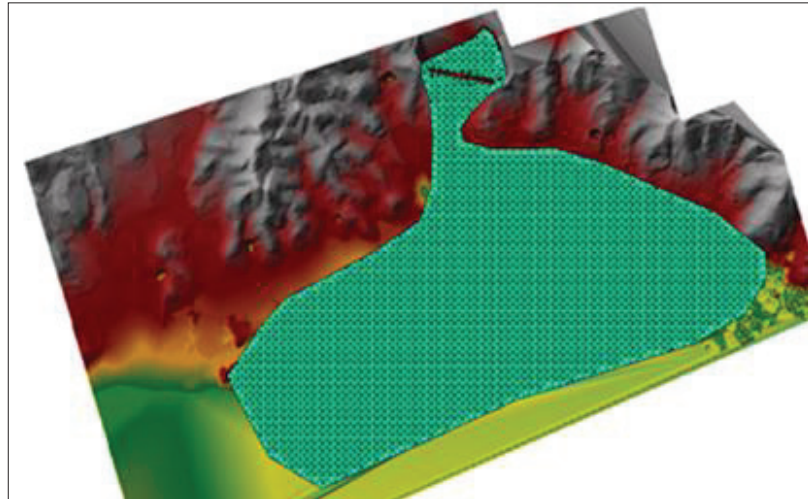
Figure 4.15 2D Inundation Area and Dam Reservoir

As upstream boundary condition the flood hydrograph was used too. The highest depth was 2.6 m at experiment and 3.5 m at simulation. The highest velocity was 2.9 m/s at experiment and 4.75 m/s at 2D simulation. Both velocity and depth were analyzed at Location 4 (given in Chapter 3) right downstream area because experimental study had accurate results. Depth and velocity graphs are given in the Figures 4.16 and 4.17.
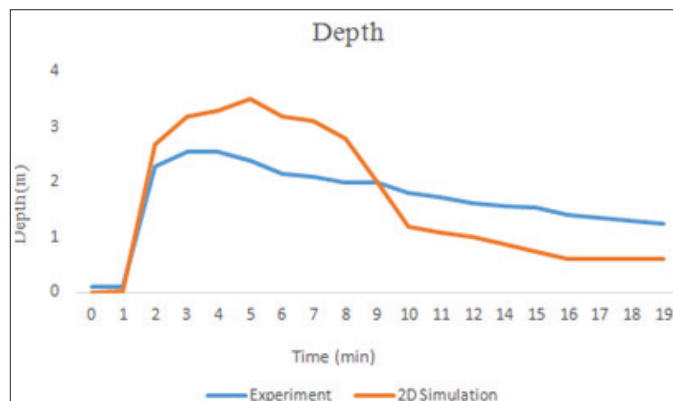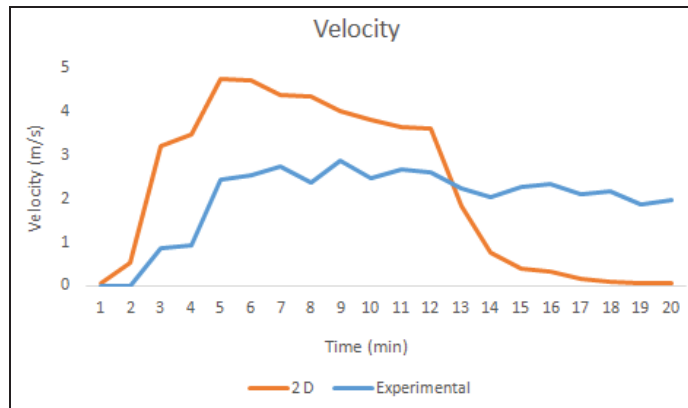

Figure 4.16: Depth Comparison

Figure 4.17: Velocity Comparison

The Figure 4.18 represents the water depths after 2D simulation at 2nd minute. Depths varied 0.24 m downstream to 6.25 m upstream. water could not reach some higher elevated area. The highest water depth encountered right in front of the dam gate. 280 ha area was inundated.
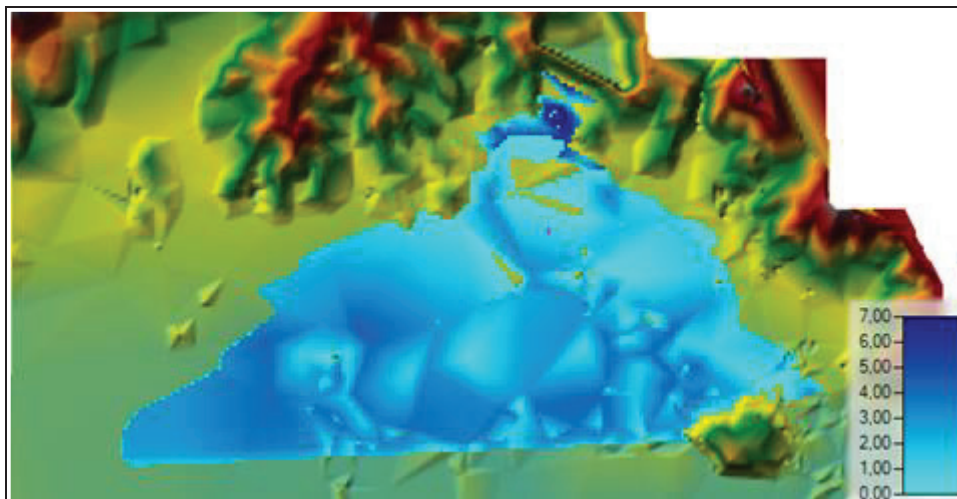

Figure 4.18: Depth Profile

According to simulation water was completely reached settlement area and most of the buildings would be taken damages from flood. At least building first floor would be inundated too and in the 2D simulation 300 ha area would be inundated. In the 2.5

minutes, flood have already reached settlement and highway, was critical for transportation the area. Water propagation were given in the Figures from 4.19 to 4.24. According to simulation water was completely reached settlement area and most of the buildings would be taken damages from flood. At least building first floor would be inundated.
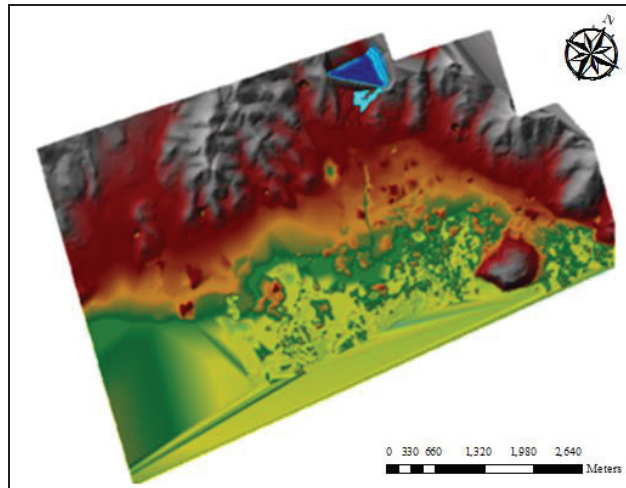

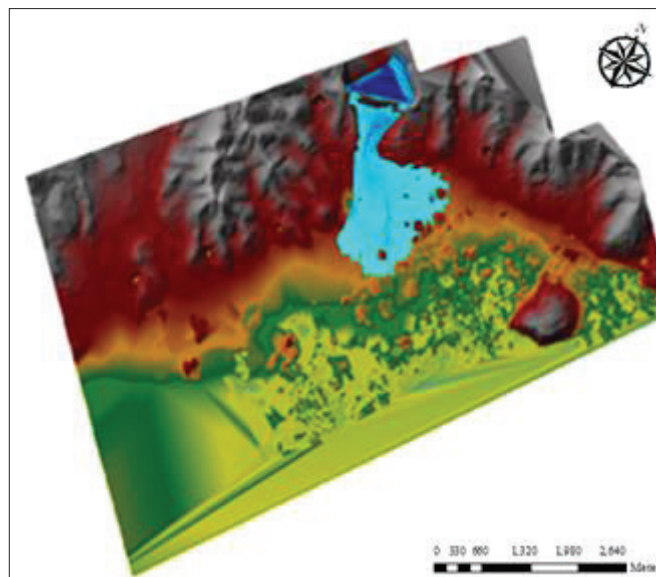Figure 4.19: Water Propagation at 15 sec

Figure 4.20: Water Propagation at 25 sec
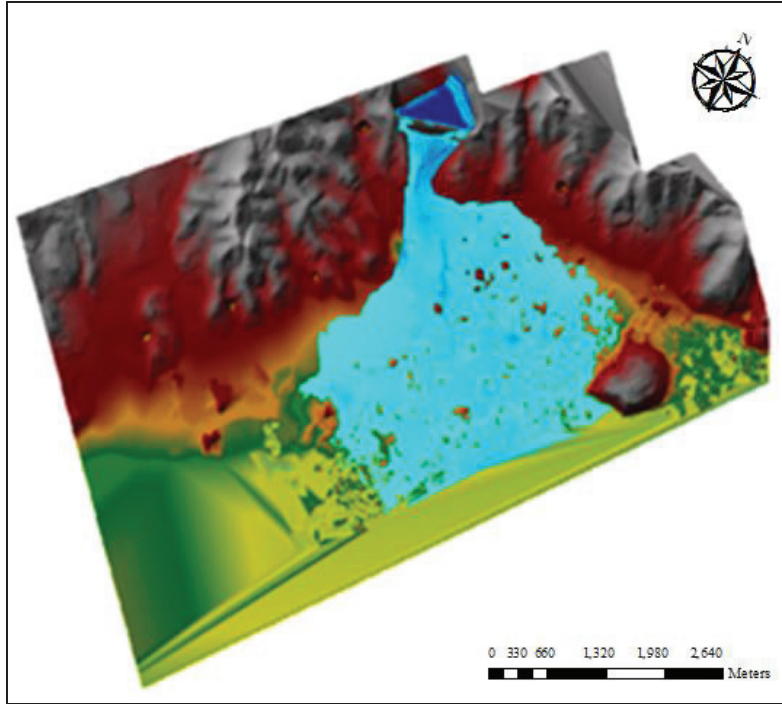
Figure 4.21: Water Propagation at 40 sec
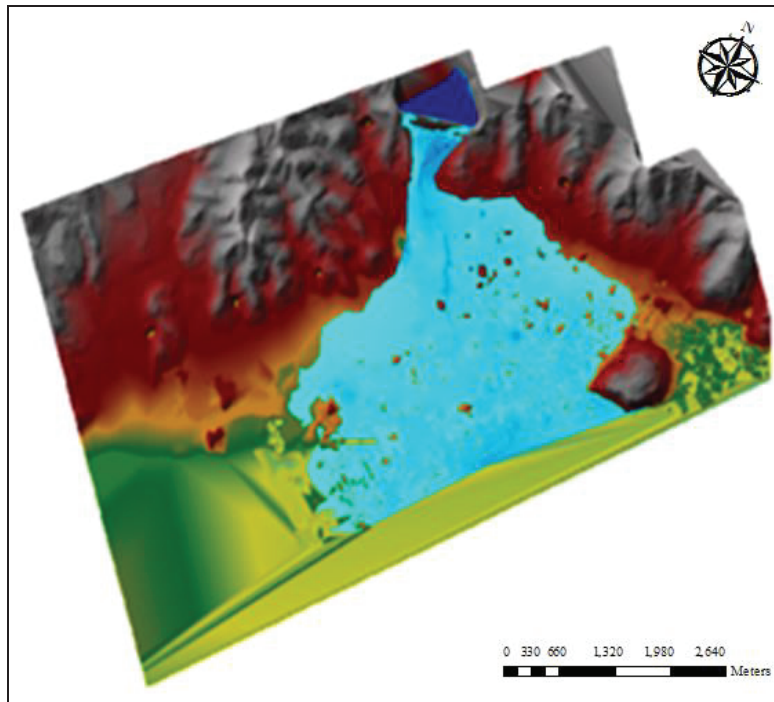
Figure 4.22: Water Propagation at 1.5 min
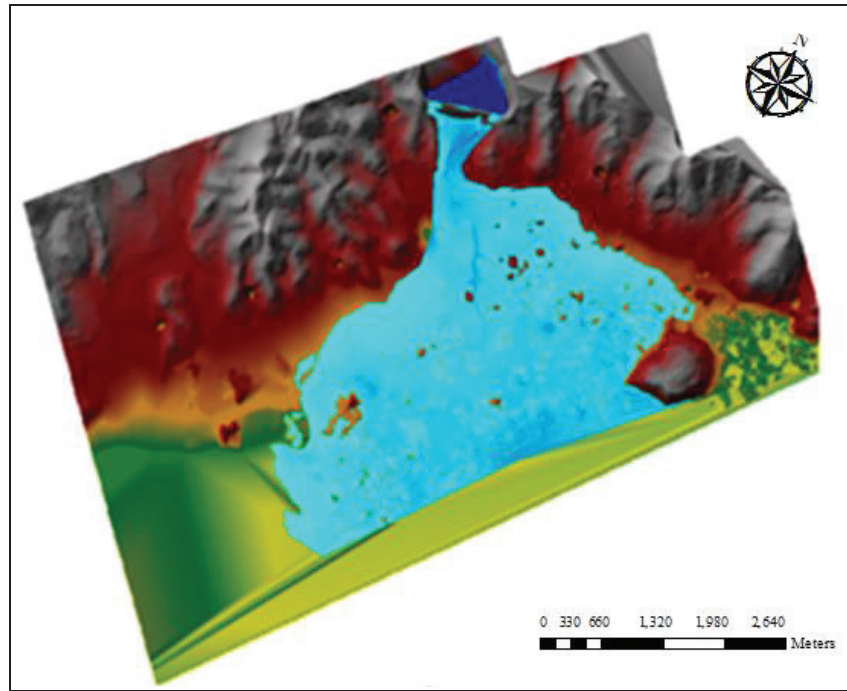
Figure 4.23: Water Propagation at 2 min

Figure 4.24: Water Propagation at 2.5 min

45

Figure 4.25 gives the velocity profile at 3rd minute. The velocity varied 0.24 m/s to 28.1 m/s. The maximum velocity occurred at 1.5 minutes. The highest velocity was seen near to dam gate. The lowest velocity was seen at downstream on left side.

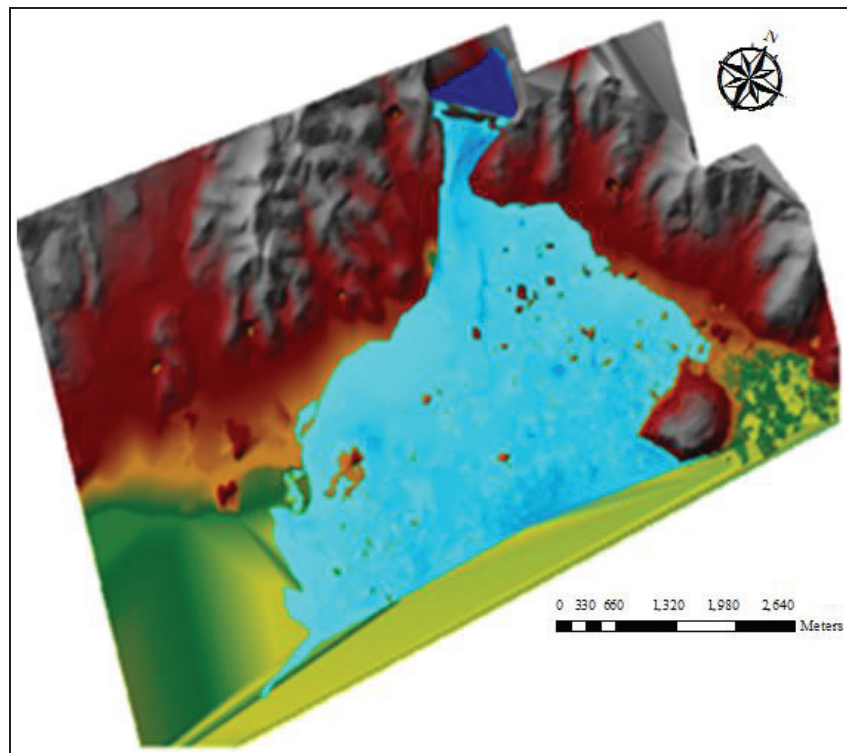Figure 4.25: Detailed Velocity Profile

CHAPTER 5

COMPARATIVE STUDY

Input data is very important for both models. DEM is required for both case but 1D model can be created also without DEM. While the geometric configuration is based on the cross-sections in the 1D model, 2D model relies on finite element mesh resolution. In this study DEM is used for both cases because cross sections and other geometric characteristics of study area is acquired from DEM. For the 1D model used for simulation; stream centerline, flow paths, banks, cross sections, and land use type were created in Hec-GeoRAS. On the other hand, 2D mesh, weir parameters, inlet, dam bridge data were created in HEC-RAS for 2D modeling. All geometric data created based on the same DEM.

During the floodplain, momentum equations for 1D model and wave equations for 2D model were used. In 2D modelling, full momentum equation can be used also, but energy losses were occurred. The results have been compared with required data for simulation, data preparing process, inundated area, flood depth and flood velocity of flood waves.

Inundated area was 280 ha according to 1D model but inundated area was executed as 300 ha in 2D model. The figure illustrates: Figure 5.1 and Figure 5.2 present inundation areas, respectively, obtained using 1D and 2D models. Figure 5.3 shows the estimated overlapping flooding areas.

Also, maximum flood depth in upstream reached to 4.21 m and 1.94 m in the downstream in 1D model simulation where the maximum flood depth was 3.5 m in upstream area and 0.24 m in the downstream according to 2D simulation. Figure 5.4 shows the flow depths change in time at upstream.
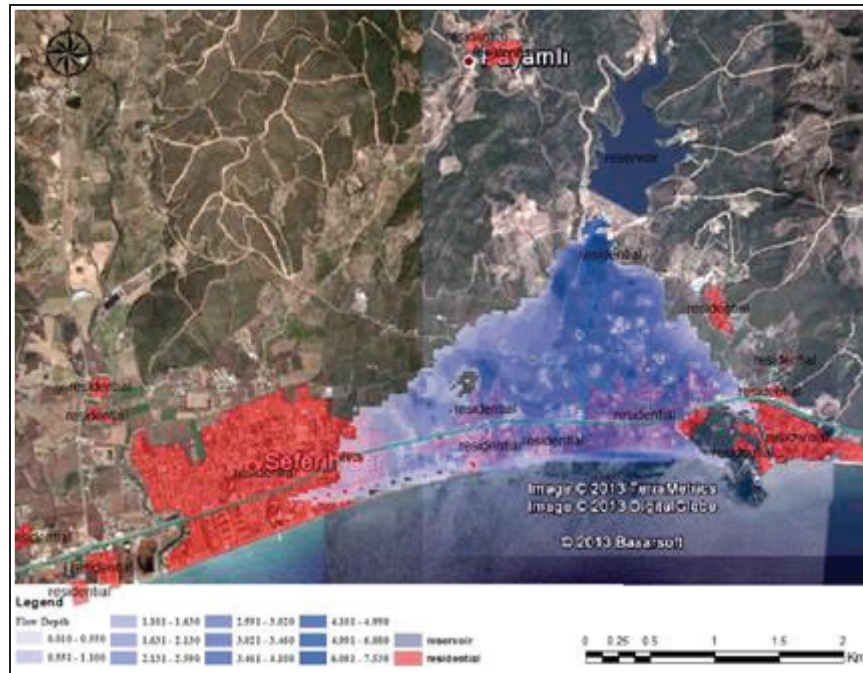
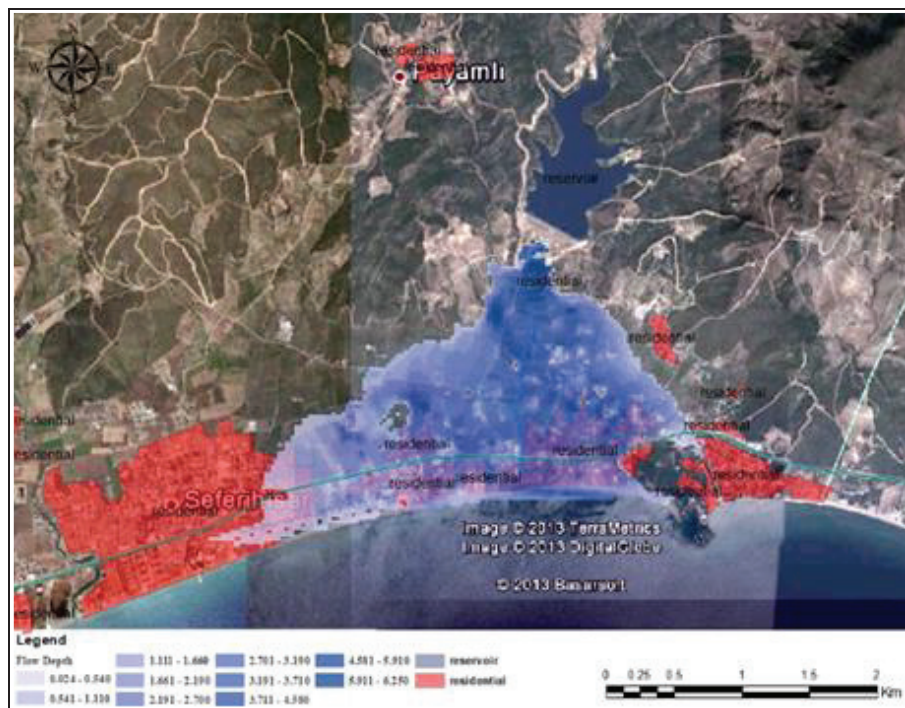Figure 5.1 Inundation area predicted by the 1D model

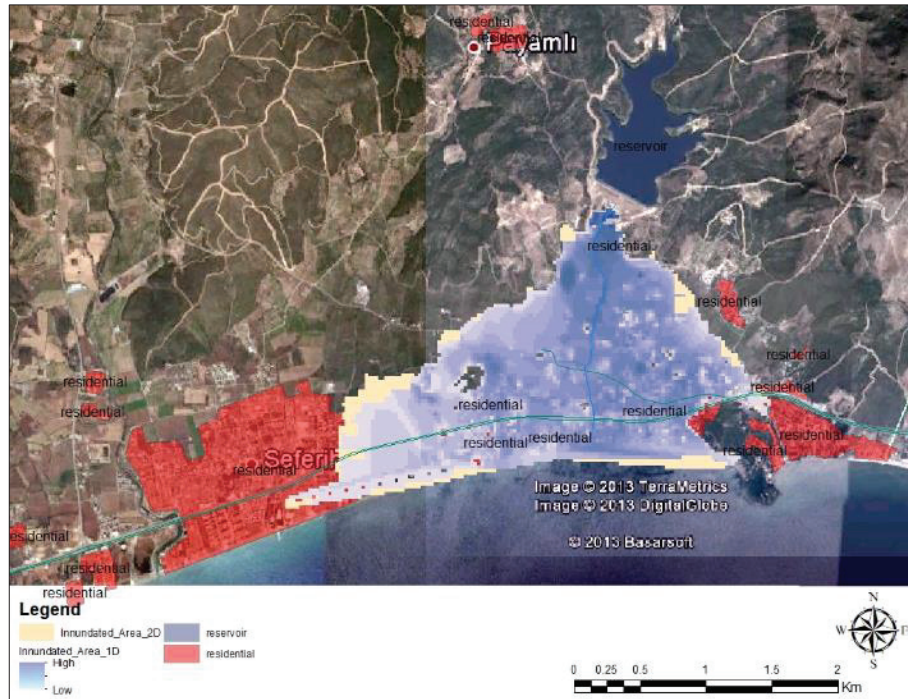Figure 5.2 Inundation area predicted by the 2D model

Figure 5.3 Overlapped inundation areas predicted by 1D and 2D models
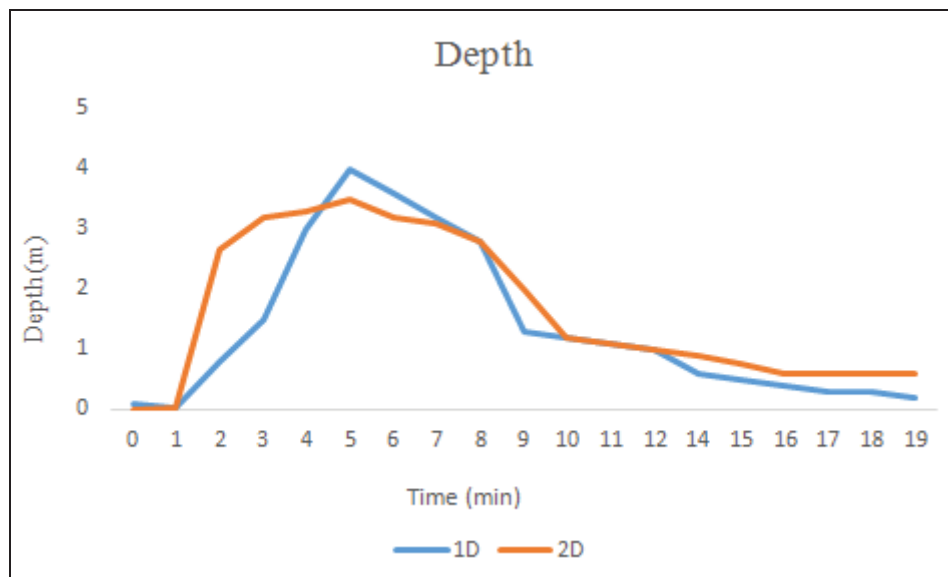
Figure 5.4 Flow depth profile at upstream

The highest flow velocity was observed on right side (flow direction) at a distance of about 280-300 meters from reservoir and flood velocity varied from 13.06 m/s to 0.018 m/s in 1D model simulation. The maximum velocities were reached in about 2.5 minutes in 1D model and in 2D model simulations. Following Figures 5.5 and 5.6 show flow velocity at upstream and downstream area for both models. Accordingly 2D model simulation, the highest velocity was observed on the right side (flow direction) at a distance of about 300 meters from the storage area and flood velocity varied from 28.1 m/s to 0.24 m/s.
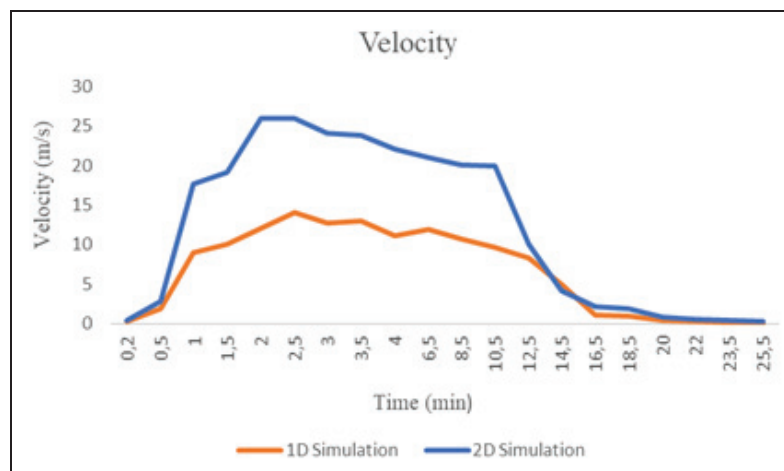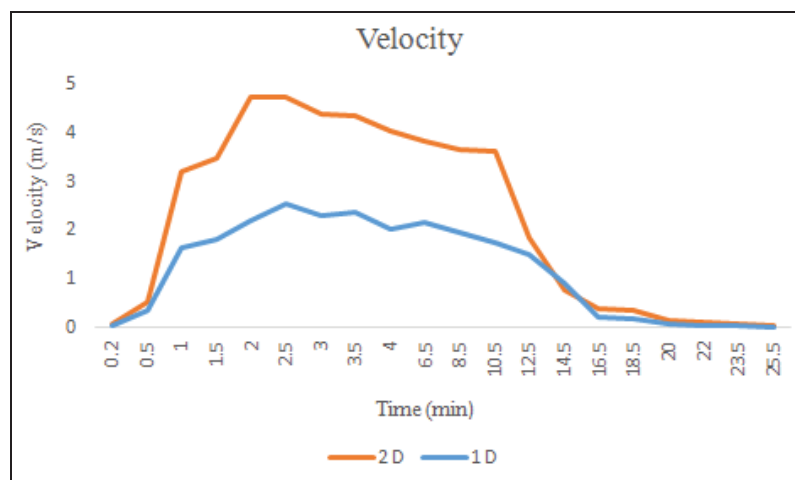

Figure 5.5 Velocity profile at upstream

Figure 5.6 Velocity profile at downstream

CHAPTER 6

CONCLUSIONS

The aim of this study is to assess Ürkmez Dam failure potential risk with dam breach analysis by comparing performance of 1D and 2D simulations. Begin with, physical models have high importance for calibration of both 1D and 2D modelling of dam breach. The one-dimensional model needs more detailed input data, so the data preparation period takes a longer time. Simulation results show that the areas to be submerged are approximately the same. However, the estimated size of the inundated area in the 2D model is about 5 percent larger. At the same time, the depth observed in 1-dimensional model is higher than the 2-dimensional simulation results, but the time to reach the maximum speed is slower than the 2-D model. The Table 6.1 summarize the advantages and disadvantages of 1D and 2D modeling.

To sum up, this study has evaluated performance of 1D and 2D models in HEC-RAS. Important design consideration was clarified. Ürkmez Dam is a small dam which is 30 m far from sea. For the detail analyzing performance comparison of 1D and 2D, bigger dam can be chosen. Also, physical model can be improved by the studies with implemented roughness concept. In this study, contour map was a unified map so some problems occurred on coordinate systems. Data processing, sensitivity analysis, calibration, stability and instability cases, and accuracy can be checked for 1D model on a larger model. Suitable cell size, cell configuration, time steps and sensitivity parameters can be checked for 2D. Also, model calibration can be improved. Manning's coefficient, boundary and initial conditions can be investigated with detailed information related to dam, river and environment.

Table 6.1: Summarize the advantages and disadvantages of 1D and 2D modeling

Data requirement and preprocessing needs	1D	2D
Cross section (XS) data	Yes	No
Digital Elevation Model (DEM)	Yes	Yes
River bathymetry interpolation	No	No
Data preperation	Long	Short
Hec-GeoRAS	Yes	Yes
Input data	More	Less
Geometry Set-up		
Terrain represented by	XS	Mesh
Set-up time	Suitable	Depending
Computations		
Computation time	Short	Long
Stability problems (instability source)	XS placement	Full momentum in river, bridges etc.
Results		
Depth	Higher	Lower
Velocity	Lower	Higher
Inundation Area	Less	More

REFERENCES

1. Biondini, F. & Frangopol, D.M. 2016. "Life-cycle performance of deterioring strcutural systems under uncertainity: Review." Journal of Structural Engineering 142(9): F40116001.

2. The International Disaster Database, Centre for Research on the Epidemiology of Disasters (CRED). "Annual Disaster Statistical Review" 2016, p. 51.

3. Kaya, Ç.-M. "Akım Gözlem İstasyonu Bulunmayan Taşkın Havzalarındaki Değişimlerin Taşkın Riskine Etkisinin Belirlenmesi: Rize, Güneysu Örneği." PhD thesis, Karadeniz Technical University, Trabzon, (2017).

4. Bozkus, Z. (2003). "Pre-Event Failure Analyses of Kestel Dam for Disaster Management." J. of Physical and Engineering Science, ARI, The Bulletin of the Istanbul Technical University, Istanbul, Turkey, Vol. 53 No. 2.

5. Yanmaz, A.M., and Beşer, M.R., (2005). "On the Reliability-Based Safety Analysis of the Porsuk Dam", Turkish Journal of Engineering and Environmental Sciences, Tubitak, 29 (5), 309-320.

6. Molu, M. 1995. "Dam-break flood in a natural channel: A case study." MS Thesis, Civil Engineering Department, Middle East Technical University, Ankara, Turkey.

7. Chanson, H. (2010). "Application of the method of characteristics to the dam break wave problem." Journal of Hydraulic Research, Vol. 47.

8. NASA Images. (2002). https://earthobservatory.nasa.gov/images/2508/flooding-caused-by-the-collapse-of-the-zeyzoun-dam-syria

9. Alcrudo, F., Mulet, J.(2007). "Description of the Tous Dam break case study." Journal of Hydraulic Research, Spain.

10. Alcrudo, A., Mulet, J. (2007). "Tous Dam is the last flood control structure of the Júcar River." Journal of Hydraulic Research.

11. Alcrudo, F. (2003). "The Search for a Test Case. IMPACT Project." Louvain-La-Neuve, Belgium.

12. Yochum, S. E., Goertz, L. A., and Jones, P. H. (2008). "The Big Bay Dam failure: Accuracy and comparison of breach predictions." J. Hydraul.Eng.,

13. Lemichhane, N., Sharma S. (2017). "Development of flood warning system and flood inundation mapping using field survey and LiDAR Data fort he Grand River near the City of Painesville." Ohio. Hydrology (Open Access journal).

14. Lavoie, B., Mahdi, T.-F. (2017). "Comparison of two-dimensional flood propagation models: SRH-2D and Hydro_AS-2D. Natural Hazards." p.1207-1222.

15. Almassri, B. "Numerical simulation analysis of dam breaks using ISIS & HEC-RAS" Master thesis, University of Bradford, The United Kingdom (2011).

16. Zhu, Y., Visser, P.-J., Vrijling J.K. (2004). "Review on embankment dam breach modeling." DOI: 10.1201/9780203020678.ch147. (2004)

17. Testa, G., Zuccala, D., Alcrudo, F., Mulet, J., and Frazao, S. S. (2007). "Flash flow experiment in a simplified urban district." J. Hydraul. Res.,45, 37–44.

18. Larocque, L., Imran, J., and Chaudhry, M.(2013). "Experimental and numerical investigation of two-dimensional dam-break flows." J. Hydraul. Eng.

19. Xu, F., Yang, X., Zhou, J., Hao, M. (2013). The Scientific World Journal. Vol. 2013. Article Id. 272363.

20. Güney, M.S, Tayfur, G., Bombar, G., Elçi Ş. (2014). "Distorted Physical Model to Study Sudden Partial Dam Break Flows in an Urban Area." American Society of Civil Engineers. DOI:10.1061/(ASCE)HY.1943-7900.0000926.

21. Chow, V.T.; Maidment, D.R.; Mays, L.W. (1988). Applied Hydrology, 0-07-039732-5 McGraw-Hill, New York.

22. Maidment, D.R. (1993): Handbook of Hydrology, 0-07-039732-5, McGraw-Hill, New York

23. Brunner, G.W., Piper S.S., Jensen, M.R., Chacon, B. (2015)." Combined 1D and 2D hydraulic modelling within HEC-RAS," World Environmental & Water Resources Congress, ASCE, EWRI, May 2015, Austin, TX.

24. Bulu, A. (2004). Istanbul Technical University, Lecture Note, İstanbul, Turkey.

25. Chow, V.T. (1959). Open Channel Hydraulics, McGraw-Hill Book Company, NY.

26. Cowan, W. L., 1956. "Estimating Hydraulic Roughness Coefficients." Agricultural Engineering, p.37, 7, 473-475.

27. French, R.H., Miller, J.J., Dettling, C., Carr, J.R., 2006. "Use of Remotely Sensed Data to Estimate the Flow of Water to a Playa Lake." Journal of Hydrology. P. 3, 25, 67-81.

28. Yalın, M., S., (1971). Theory of hydraulic models. London: The Macmillan Press Ltd.